HIGH TEMPERATURE, BURIED PERMANENT MAGNET,

BRUSHLESS DC MOTOR

A Thesis

by

ZHENGXIN ZHANG

Submitted to the Office of Graduate Studies of
Texas A&M University
in partial fulfillment of the requirements for the degree of

MASTER OF SCIENCE

August 2010

Major Subject: Mechanical Engineering

High Temperature, Buried Permanent Magnet, Brushless DC Motor

HIGH TEMPERATURE, BURIED PERMANENT MAGNET,

BRUSHLESS DC MOTOR

A Thesis

by

ZHENGXIN ZHANG

Submitted to the Office of Graduate Studies of
Texas A&M University
in partial fulfillment of the requirements for the degree of

MASTER OF SCIENCE

Approved by:

Chair of Committee,	Alan B. Palazzolo
Committee Members,	Miladin Radovic
	Thomas W. Strganac
Head of Department,	Dennis O'Neal

August 2010

Major Subject: Mechanical Engineering

ABSTRACT

High Temperature, Buried Permanent Magnet, Brushless DC Motor. (August 2010)

Zhengxin Zhang, B.S., Shanghai Jiao Tong University

Chair of Advisory Committee: Dr. Alan B. Palazzolo

A high temperature magnetic bearing system using high temperature permanent magnets from Electron Energy Corporation (EEC) is under development. The system consists of two radial bearings, one thrust bearing, two radial catcher bearings and one motor. The purpose of this research is to develop one of the critical components of the system, namely, the High Temperature Permanent Magnet motor.

A novel High Temperature Permanent Magnet (HTPM) Brushless DC(BLDC) motor capable of operating at 1000°F (538°C) is designed. HTPMs developed at Electron Energy Corporation are buried into the rotor. The high temperature motor is designed to produce 5.1kw of power at a top running speed of 20000 rpm. The numerical values of the motor voltage, power and torque output are predicted from calculations of the nonlinear finite element model of the motor. The motor stator is wound, potted, cured and high potential tested at 1000°F.

A servo amplifier from Advanced Motion Control is used to drive the high temperature motor. High temperature displacement sensors are set up for sensing the rotor position to form a closed loop motion control. However, the noise problem of the high temperature sensors causes a failure of this approach. An open loop approach is then developed and this approach succeeds in spinning the rotor with the capability of self-

starting.

The status of the full system assembling is introduced. Some other components of the system are briefly presented.

ACKNOWLEDGEMENTS

NOMENCLATURE

EEC   Electron Energy Corporation

VCEL   Vibration Control and Electromechanics Lab

PM   Permanent Magnet

HTPM   High Temperature Permanent Magnet

PWM   Pulse-Width Modulation

DSP   Digital Signal Processing

K-Map   Karnaugh Map

AMC   Advanced Motion Control

BPM   Buried Permanent Magnet

TABLE OF CONTENTS

LIST OF FIGURES

Page

Page

LIST OF TABLES

1. INTRODUCTION

1.1 Overview

The Electron Energy Corporation (EEC) along with the National Aeronautics and Space Administration (NASA) is conducting research on magnetic bearings. The purpose of this research is to design and develop a high temperature (1000ºF) Magnetic Bearing System using High Temperature Permanent Magnets (HTPM), developed by the EEC. This high temperature magnetic bearing system would be used in high performance, high speed and high temperature applications like space vehicles, jet engines and deep-sea equipments. The bearing system has a target design to carry a load equal to 500 lb-f (2225N). The entire system will consist of two Radial Bearings, one Thrust Bearing, one Permanent Magnet Brushless DC Motor and two Catcher Bearings.

The high temperature motor is designed to work in a high temperature (1000°F), and also is expected to produce power in the range of five to ten horsepower (3.75 kw to 7.5 kw) and reach the top running speed up to 20000 rpm. The motor can achieve self-starting with a standard three-phase control. High potential test is performed to justify the high temperature capabilities. A test stand is built to verify the motor drive and self-starting capability.

This high temperature motor utilizes EEC high temperature T550 magnets and VCEL high temperature electric coils which are capable of operating at 1000°F (538 °C).

_____

This thesis follows the style of Journal of Vibration and Acoustics.

EEC has unique capabilities in developing High Temperature Permanent Magnets (HTPMs) for motor/generator/magnetic bearing/solenoid applications. The recently developed and patented high temperature magnets (U.S. Patent number: 06,451,132) have a straight-line extrinsic demagnetization curve up to 562ºC, which makes possible the design of high temperature magnetic bearing system using PMs. Integration of these magnets will provide higher efficiency and reliability for the magnetic suspensions as well as reduce the required electronics. The typical demagnetization curves of EEC T550 high temperature magnets are shown in Fig. 1-1. As temperature grows the magnetic strength decreases.
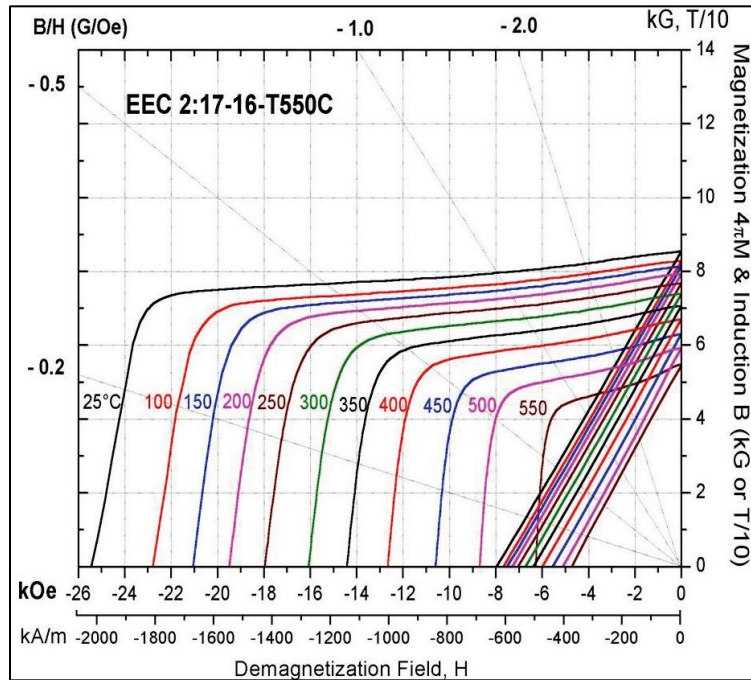
Fig. 1-1 Typical Demagnetization Curves of EEC High Temperature Magnets

1.2   Objectives

- Build a high temperature, buried permanent magnetic, brushless DC motor

- Build a commutation circuit for driving the motor utilizing the high temperature displacement sensor to run the motor at low speed and justify the self-starting capability.

- Help build the universal magnetic bearing test rig

1.3   What Is the Novelty?

A novel feature of this brushless DC motor is that it is designed to operate in a high temperature 1000°F (550°C) hostile environment and it utilizes a rotor in which high temperature permanent magnets are buried. Based on the author's review of the literature, this is the first permanent magnet high temperature motor.

1.4   Significance

Most motors and actuators are not designed to survive high temperature environments. The elevation of temperature is a major reason that causes motor failure. For common motors, problem of high ambient temperature is the insulation deterioration. Elevated temperatures may cause insulation to become brittle. Also, many bearing failures of the motors are a result of the motors exceeding their temperature limits.

One may ask if there is a need for high temperature motors. The answer is there are

many applications that require a motor bearing system that works in an extreme temperature environment. A regular motor does not have such ability to survive high temperature, such as jet engines or deep sea drilling equipment. The high temperature motor is necessary in such applications. Here is a list of possible applications of extreme temperature motors.

- pumps and valves for liquid metal cooling systems

- material lifting from oil and geothermal wells

- gimbals for expendable launch vehicle engines and components of spacecraft that operate near extremely hot sources such as the Sun.

- gas turbine starters/generators for aircraft engines

- robotic exploration vehicle systems that operate in and around terrestrial volcanoes and deep ocean hydrothermal vents

1.5   Literature Review

As a part of the high temperature magnetic bearing system, the high temperature motor plays an important role. By modifying an eight-pole radial magnetic bearing, NASA Glenn Research Center and Texas A&M University developed and tested a switched-reluctance electric motor, which was capable to run as high as 8000 rpm at temperatures up to 1000°F (540°C) [1]. The unique features of this motor were its electromagnet coils. Honeybee Robotics developed and demonstrated a first-generation prototype of an extreme temperature, high-pressure (~90 bar) motor for possible future use on the surface of Venus. A small switched-reluctance type motor, which operated

without permanent magnets, was built and successfully tested at temperatures up to 460°C [2]. High temperature superconducting motors have a great advantage in weight, power density, and efficiency in comparison to conventional motors [3].

However, all of the high temperature motors mentioned above do not include any permanent magnets. Recently, buried permanent magnet (BPM) motors, often referred to as interior permanent magnet (IPM) motors, have become more commonplace. In addition, a reluctance torque is generated which increases the motor efficiency. There are several advantages, including an air gap length that may be small compared with those in the other types of motors and the buried structure design will effectively protect the magnets. Also, using the permanent magnets can reduce the power loss on the coils.

2. HIGH TEMPERATURE MOTOR DESIGN

2.1 Mechanical Design

The EEC motor is designed to produce power in the range of 5 to 10 horsepower (3.75 kw to 7.5 kw). The top running speed is 20000 rpm. It is designed to be self-starting with a standard three-phase controller. Peak current and voltage drawn by the motor are 10 Amps and 240 Volts. The motor is also designed for a high power to weight ratio with high temperature operating conditions. The motor is a brushless DC motor with six poles on the stator and four poles on the rotor.

Laminates Stack
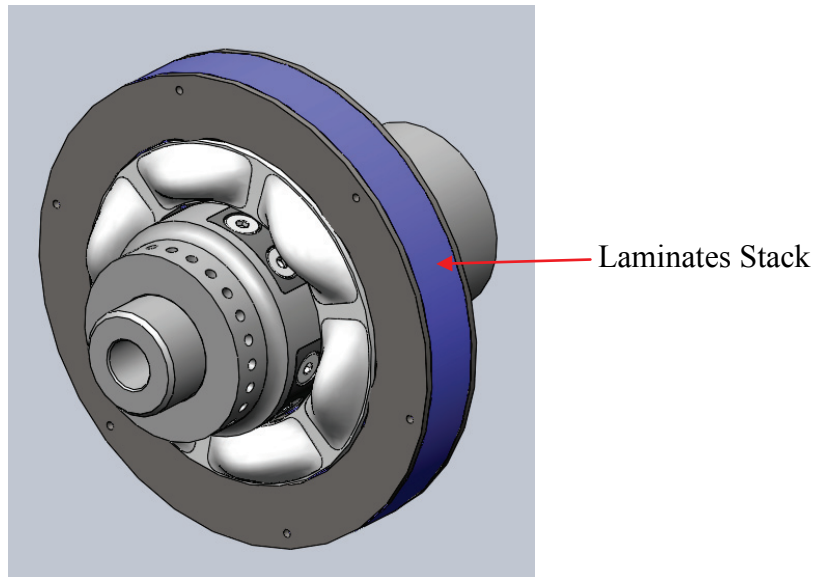
Fig. 2-1 Solidworks Model of High Temperature Permanent Magnet Motor

A Solidworks model of the rotor is shown in Fig. 2-1. The permanent magnets are buried in the rotor which can not be seen from outside and the coils are also covered with

ceramic potting which protects the coils. The laminates stack of the stator is indicated in the figure. More details of the motor stator and rotor designs are illustrated in the following sections.

2.1.1 Rotor Design

The rotor of the motor has T550 Magnets imbedded below the surface. The design of buried magnets minimizes the damages of the magnets caused by the initial levitation of the rotor and hard magnetic bearing landing. When the rotor reaches a high rpm, the embedded magnets are protected from the rotating stresses by the high strength rotor that encases them.
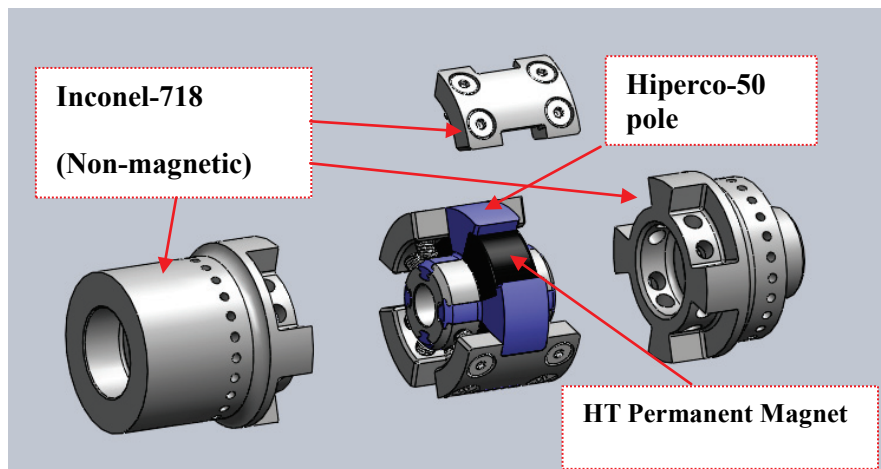
Fig. 2-2 Exploded View of Rotor

Fig. 2-2 gives a close look of how the magnets are buried. There are four T550 magnets in the rotor which are magnetically oriented so that the flux flows

circumferentially through them. The north-south orientation of the embedded magnets alternates around the rotor. In other words, each magnet is oriented to repel the two magnets adjacent to it. As stated before, there are four poles on the rotor, two north poles and two south poles. To generate these four poles, the rotor is made of two materials, Hiperco-50 (cobalt-iron-vanadium alloy), which has high permeability and Inconel-718, which limits the magnet flux. In between the magnets, one may see the segments which are laminates stack of Hiperco-50. This arrangement generates four poles symmetrically distributed on the surface of the rotor (Fig. 2-3). Fig. 2-4 shows a picture of the rotor before assemble with the stator.
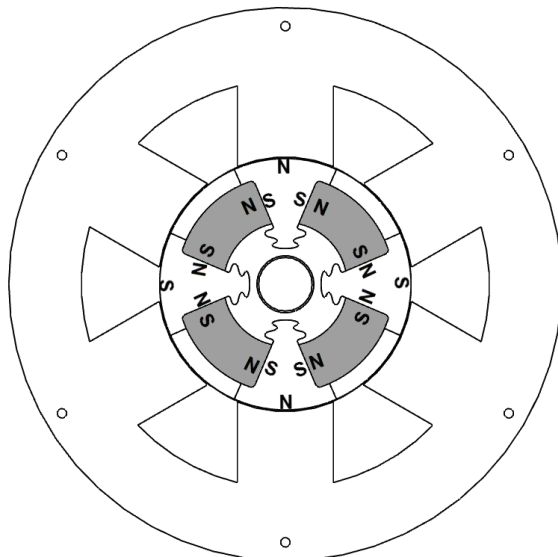
Fig. 2-3 Arrangement of the Magnets

Fig. 2-4 The Rotor

2.1.2   Stator Design

The stator is a laminates stack of Hiperco-50 which is a high permeability cobalt-iron-vanadium alloy. There are no permanent magnets in the stator while each of the six poles has a coil wound. It is connected in such a way that coils on stator poles, separated by 180°, are wired together in series. Thus, the six poles are divided into three electric coil pairs which are considered the three phases of the motor, each of which carries one phase of alternating electric current.

The coils are wound by hand in the lab using high temperature wires. Unlike regular motors, the coils are not directly exposed to the air, otherwise the fiber coating on the high temperature wires will detach at 1000 °F, which leads to a coil break down at high voltage. The VCEL at Texas A&M University developed unique bobbin and potting techniques that can prevent such problems.

The laminated stator and the coil winding are shown in Fig. 2-5 and Fig. 2-6, respectively. In Fig. 2-6, before winding the coil, the high temperature potting material is used to cover all of the poles, insulating the wires and the stator. This procedure is the special bobbin technique for high temperature coil.

Fig. 2-5 Laminated Stator and Poles
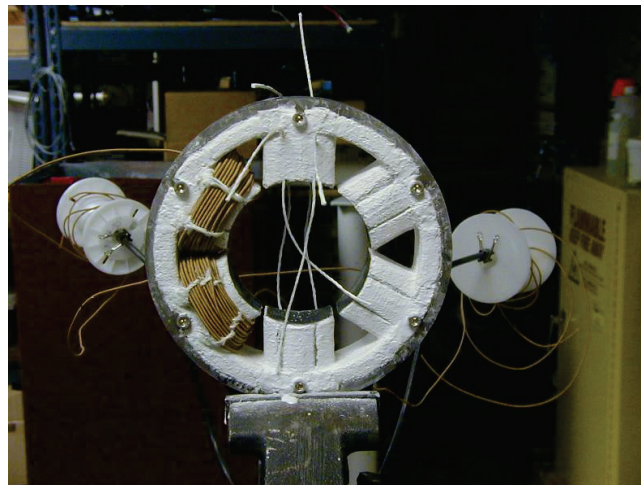
Fig. 2-6 Coil Winding

Once the coils are wound, the molding process is conducted to form the potting

cement on the stator (Fig. 2-7). A mixture of high temperature ceramic powder and water is used. Grooves are made to release the stress from thermal expansion. The stator is then placed into an oven for curing, during which most of the moisture will vaporize and the potting will be hardened. Fig. 2-8 shows the stator after curing at 300°F for 3 hours.

Fig. 2-7 Motor Stator Potting

Fig. 2-8 Motor Stator after Curing

2.1.3   Dimensions of the Motor

Table 2-1 lists the dimensions of the designed motor and Fig. 2-9 shows the corresponding sketch of the dimensions.

Table 2-1 Motor Dimensions

Stator Laminate OD(R7)	4.02 inch
Stator Laminate ID(R5)	3.70inch
Stator Length	2.50 inch
Rotor ID(R1)	1.50 inch
Rotor OD(R4)	3.66 inch
Air Gap Flux	0.45 Tesla
Air Gap	0.02 inch
Permanent Magnet ID(R2)	1.70 inch
Permanent Magnet OD(R3)	3.46 inch
Permanent Magnet Thickness	1.00 inch
Winding Style	Y
Number Turns/Coil	36
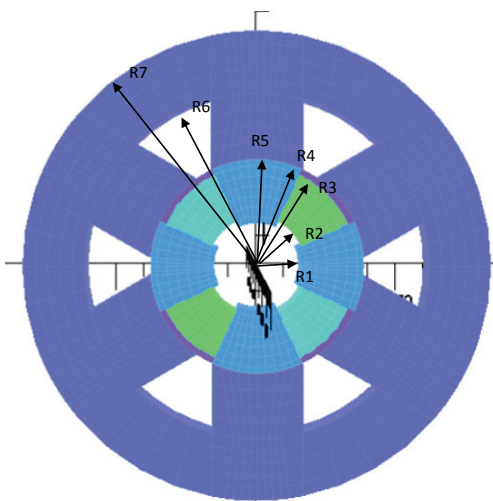
Fig. 2-9 Motor Dimension Sketch

2.2   Motor Magnetic Flux Path

According to the design of the rotor and the stator, the flux lines are simulated. The flux lines in the motor generated by the permanent magnets are shown in Fig. 2-10. Flux lines exit the rotor at the top and bottom and return to the rotor through the sides. This is also simulated with nonlinear FEA at 1000 °F (Fig. 2-11) [4].

The magnetic field generated by electric coil pairs effectively rotates around the rotor because of the synchronized three-phase currents, and the field attracts the magnetic poles on the rotor. The rotor speed is synchronized with the alternating current frequency. Timing the current phases with respect to the rotor angular position is an important issue for driving the motor, because it allows the stator to continuously generate torques in the same direction. Normally, this timing is accomplished by rotor position sensors, but, for a high temperature motor, the regular rotor position sensor such as encoder and Hall Effect sensors will fail at such a severe environment. Thus, another approach must be found and is discussed in detail in later sections.
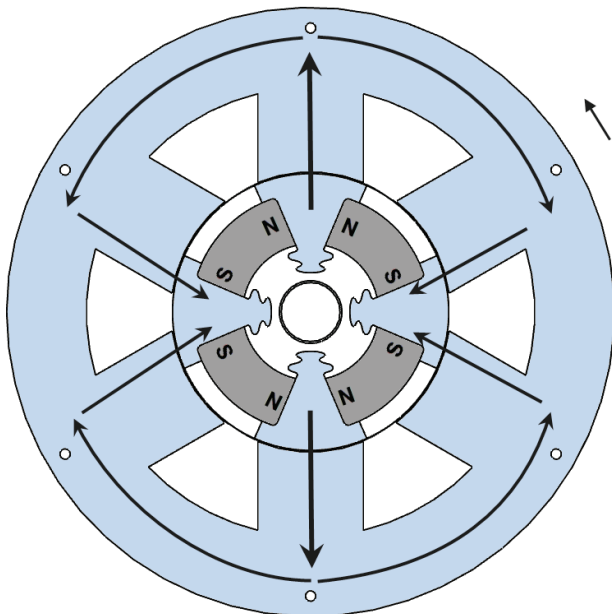
Fig. 2-10 Designed Magnetic Flux Path
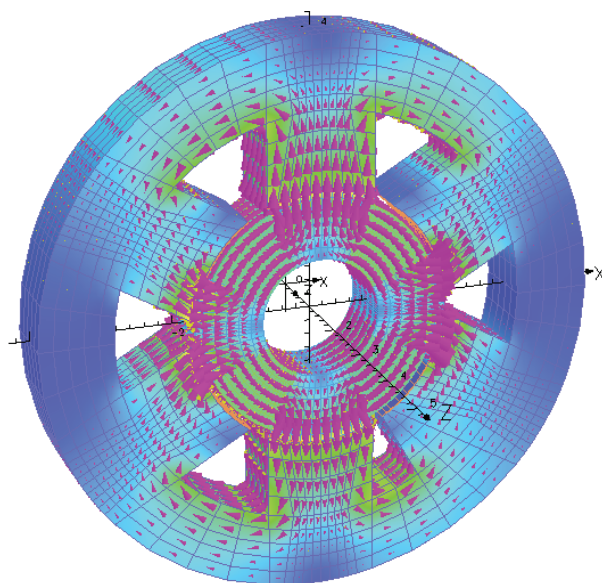
Fig. 2-11 Magnetic Flux Predicted by Nonlinear

FEA Simulation at 1000°F (540 °C) [4]

2.3   Motor Circuit Model

Predictions of the motor performance are accomplished with a closed loop electric circuit incorporating the motor. The circuit is broken down into three sub-circuits which are the equivalent generator as motor rotating, the coil pair inductor and the coil pair resistor (Fig. 2-12). These three circuits dissipate energy and the voltage will be dropped. The electronic drive serves as the source.
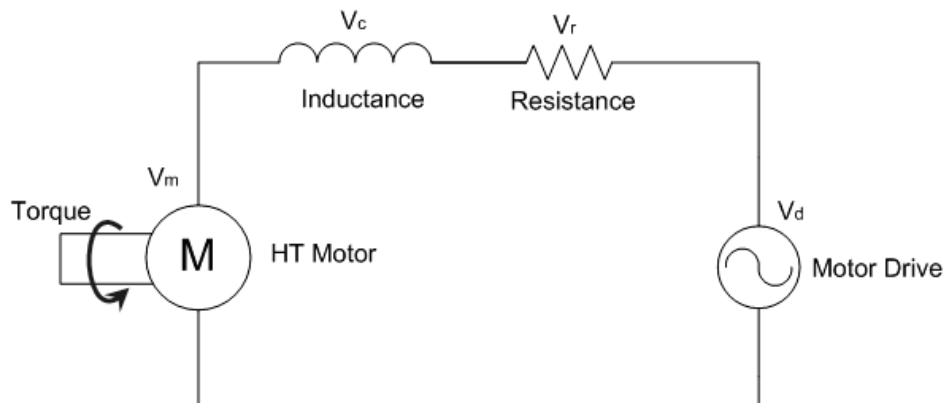
Fig. 2-12 Motor Circuit Model

The three sub-circuits are evaluated to determine their contributions on the voltage drop.

- *Motor generated voltage*

As the rotor turns, the amount of magnetic flux passing through the stator poles varies. The voltage induced by the changing of flux is the motor generated voltage which

must be compensated by the source. Measurement of this flux amount with the FEA model is made with the rotor at three different angles. A sinusoidal magnetic flux waveform through the pole is predicted as shown in Fig. 2-13. A sinusoidal variation of the flux is indicated by three separate angle calculations of the flux through the pole.
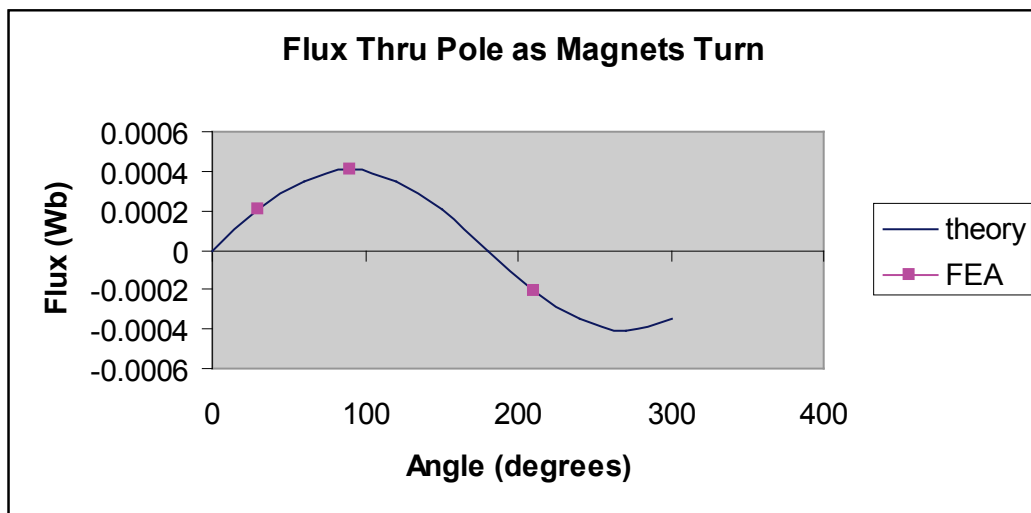
Fig. 2-13 Three Angle Calculation

The voltage induced in the coil around the pole by variation in flux is calculated from Equation (1) according to Equation (2).

$$V_m = N \frac{d\Phi}{dt} \qquad (1)$$

$$\frac{d\Phi}{dt} = \Phi \omega_e \cos(\omega_e t) \qquad (2)$$

where

Φ : Peak flux determined by FEA model

ω_e : Rotating speed in rad

N : Number of turns of the coil pair

V_m : Voltage drop due to the rotation of the motor

- ***Voltage drop across coil inductance***

The inductance of the coil is another reason of the voltage drop. In this section, the voltage drop across coil inductance due to the current from the motor controller is discussed. The motor controller sends a controller AC current to turn the rotor. This current must go against the voltage produced by the rotating magnets predicted in Equation(1). This current also sees a voltage drop due to its own AC nature as it passes through the rotor coils which have their own inductance due to the flux they produce as the drive current passes through them. The inductance of the coils seen by this current can also be calculated accurately from flux predictions of the FEA model. Fig. 2-14 shows the flux density passing through the coil and around the motor due to the current in the coil.
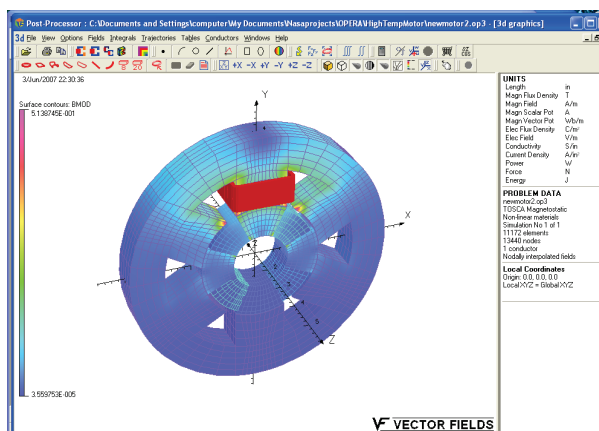
Fig. 2-14 FEA Simulation for Flux Density due to Coil Current

The corresponding coil inductance is calculated from Equation (3).

$$L_c = \frac{N\Phi_c}{I}$$

(3)

Where,

Φ_c : The flux passing through the coil due to the current

I : The current in the coil.

Since Φ_c is calculated accurately from the nonlinear FEA model, the value of the coil inductance is also determined accurately. One complication is that this inductance drops to practically zero with some rotor positions when the magnets block flux from the coil current. Thus, to get a conservative calculation of the voltage capability of the motor controller, the maximum value of the inductance is used in Equation (4). This equation gives the voltage drop seen by the controller current as it passes through the motor coil inductance.

$$V_c = L_c I \omega_e \cos(\omega_e t)$$

(4)

- *Motor coil resistance*

The current produced by the motor controller also experiences a voltage drop across the coil resistance. At 20000 rpm, the voltage drop across the coil inductance is more than 10 times higher than that across the coil resistance.

2.3.1 Motor Controller Voltage

In particular for this high temperature motor, the peak motor voltage produced according to Equation (1) is 170 V, the inductance voltage according to Equation (3) is 65 V, and the resistance voltage is 2.2 V. The two coils on opposing poles which are connected as pairs in series are considered.

The motor controller must be able to produce a steady controlled AC current by producing an AC voltage that exceeds the combined voltage drop across the coil resistance, inductance, and voltage produced by the rotor motion. For the high temperature motor presented here, this combined voltage must account for coils on poles, separated by 180°, being wired in series. This total combined voltage is predicted to be approximately 240 V when the peak current is 10 A.

2.3.2 Motor Produced Power

The power produced by the motor is the generator voltage calculated in Equation (1) times the current in the circuit which is produced by the drive. For the motor to be operating near peak efficiency, the voltage and current waveforms are timed to occur at the same moment. Since there are three phases, the peak motor power output can be calculated by

$$P_m = I \times V_m \times 3 \tag{5}$$

By plugging in the numeric values, the power is calculated.

$$10\ \text{A} \times 170\ \text{V} \times 3\ \text{phases} \ = \ 5.1\ \text{kw or 6.9 horsepower}$$

2.3.3 Motor Produced Torque

The motor torque may be calculated by dividing the power by the rotor spin speed,

$$T_m = \frac{P_m}{\omega} \tag{6}$$

Since the voltage V_m goes up proportionally to the rpm according to Equations (1) and (2), the power goes up the same way according to Equation (5). Then, dividing the power by the spin speed to get the torque indicates that the torque is not dependent on the spin speed. Torque in the high temperature brushless DC motor depends on the current as stated above.

A static torque measurement is conducted on the assembled motor rig in Section 4.

2.4 Motor Assembly

The stator and the rotor are assembled for further testing. It is supported on two journal bearings and the stator is fixed on a plate.
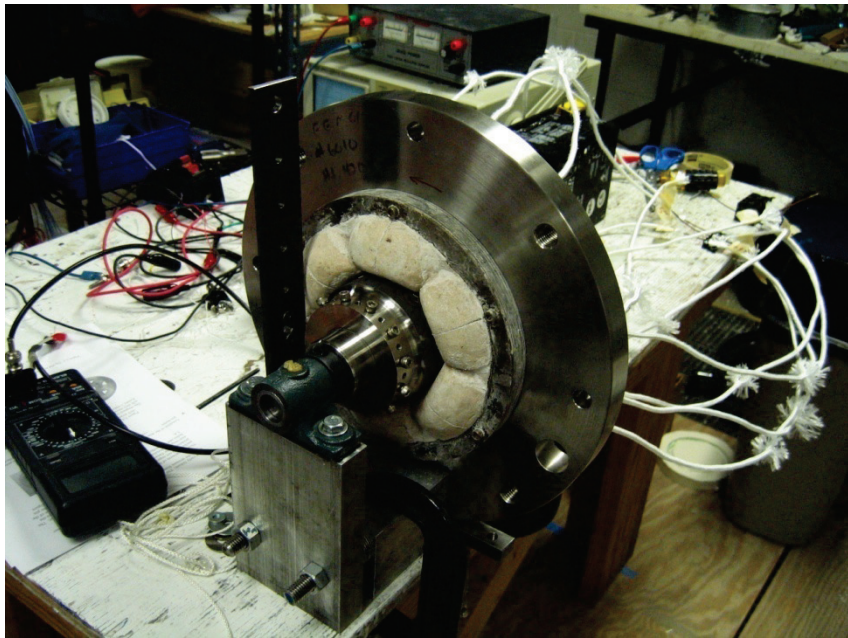
Fig. 2-15 Motor Assembly

3.   MOTOR DRIVE

3.1   Motor Operation

Based on the mechanical design, the motor has a six-pole three-phase stator and a four-pole rotor. The coils on stator poles, separated by 180°, are wired together in series shown in Fig. 3-1. Three phases are wired in a star(Y) connection so that the six poles are divided into three phases. During the conduction period of the motor operation, the DC voltage is switched between phase terminals, and the commutation sequence is AB, AC, BC, BA, CA, CB, which are shown in Fig. 3-2. This operation is called full-wave operation. In each state, two phases are conducted, leaving the third phase floating. As the switching continues, the magnetic field generated by the coil effectively rotates around the rotor, attracting the magnetic poles on the rotor to spin synchronously.
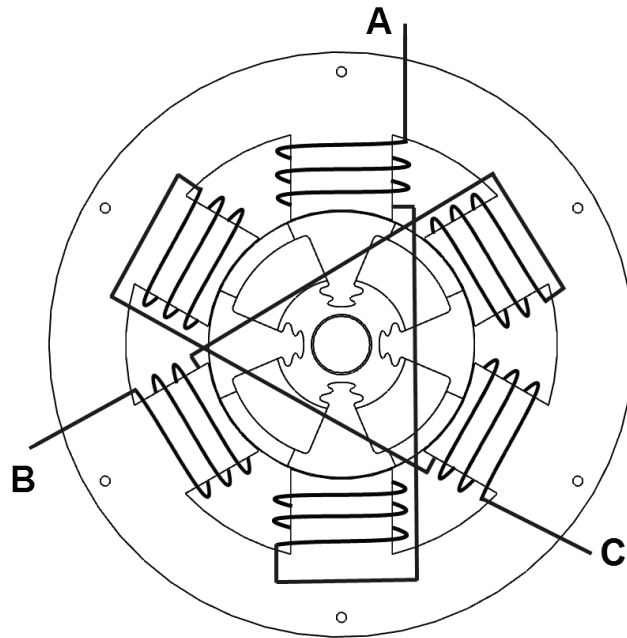
Fig. 3-1 Coil Pair Connoted in Series
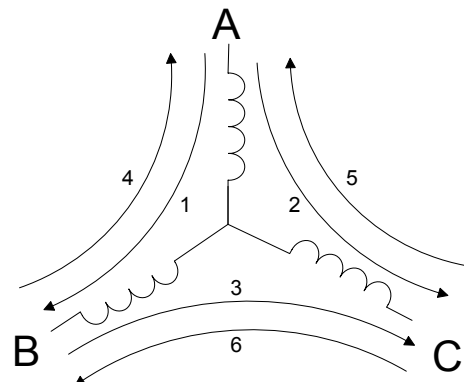
Fig. 3-2 Commutation Sequence

To achieve full-wave operation, a bridge type switching circuit (also known as three-phase IGBT drive) is utilized. S1 to S6 can be switched on and off. Each of the

power devices has a diode to guarantee current continuity. There are six states during the motor operation depending on the switching sequences. The switching process is done by the following six steps. Fig. 3-3 shows the first two steps and the current flowing paths are highlighted.

STEP1: At Electrical Angle (0° − 60°). S1, S5 are conducted.

Current direction: ＋→S1→A→B→S5→－

STEP2: At Electrical Angle (60° − 120°). S1, S6 are conducted.

Current direction: ＋→S1→A→C→S6→－

STEP3: At Electrical Angle (120° − 180°). S2, S6 are conducted.

Current direction: ＋→S2→B→C→S6→－

STEP4: At Electrical Angle (180° − 240°). S2, S4 are conducted.

Current direction: ＋→S2→B→A→S4→－

STEP5: At Electrical Angle (240° − 300°). S3, S4 are conducted.

Current direction: ＋→S3→C→A→S4→－

STEP6: At Electrical Angle (300° − 360°). S3, S5 are conducted.

Current direction: ＋→S3→C→B→S5→－

STEP7: Repeat STEP1.

IGBT Drive   Motor

(a)STEP1

IGBT Drive   Motor
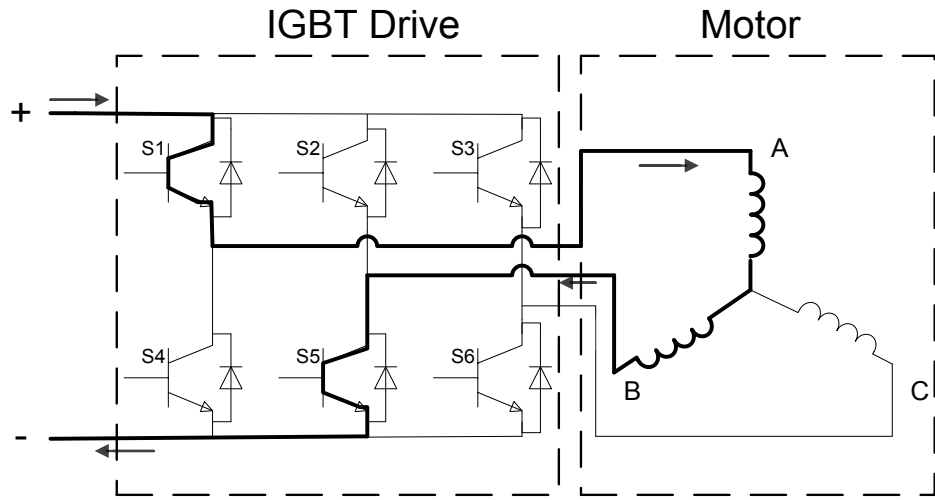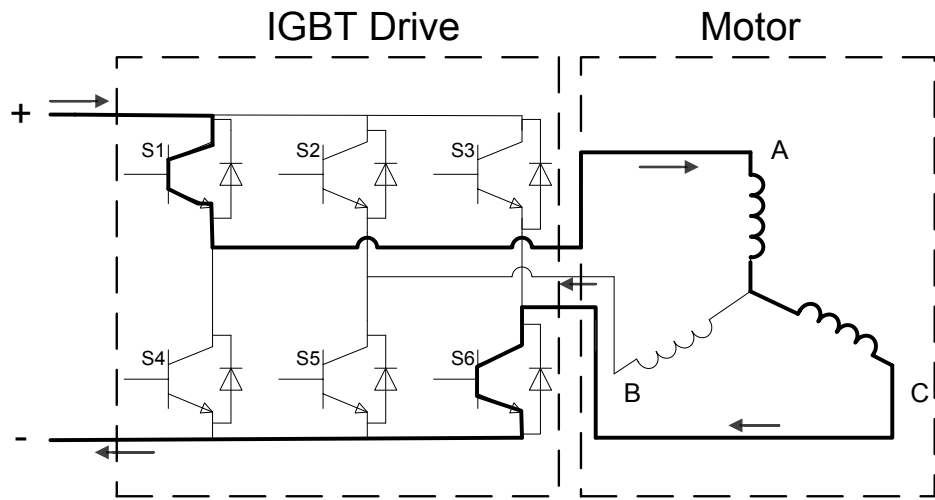
(b)STEP2
Fig. 3-3 Switching Circuit

A switching logic circuit is normally used to control the IGBT drive. In addition, a

pulse width modulation (PWM) is considered to be the most efficient and cost-effective

approach. Most servo amplifiers and microcontrollers that are commercially available for

motion control contain a PWM module. Empirically, it is required that the PWM

frequency is more than 10 times larger than the maximum operating frequency of the motor. By changing the duty cycle of the PWM signal, the speed of the motor can be changed.

3.2 Motor Commutation

The advantage of a brushless DC motor is that it replaces the mechanical commutation mechanism(commutator) with electrical commutation feedback. The commutation feedback contains the rotor magnets positions. Depending on the positions of the rotor, different coils are conducted to generate magnetic field that applies torque on the rotor. There are several ways for rotor position sensing. Hall Effect sensors, encoders and resolvers are usually used. For the high temperature motor, Hall commutation is chosen.

3.2.1 Principals of Hall Commutation

The Hall Effect sensor is a magnetic field sensor. The working principal of the Hall Effect sensor is due to the nature of a constant current in a conductor. The placement of the conductor in a stationary magnetic field creates Lorentz force that applies on moving charges and generates a voltage difference. This voltage is amplified by a differential amplifier so that it will give a high or low voltage output based on the flux direction. Thus, the Hall Effect sensor may be used as a magnetic field detector. A sketch of the Hall Effect sensor is shown in Fig. 3-4. The commercial available Hall Effect sensor is

normally fabricated into an integrated chip, combining Hall elements and differential amplifiers. (Fig. 3-5)
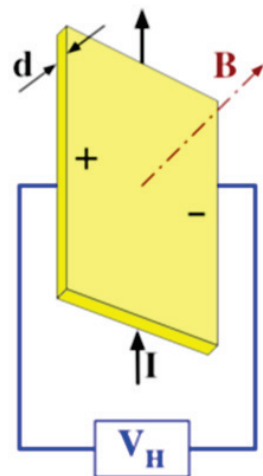
Fig. 3-4 Hall Effect Sensor Principals
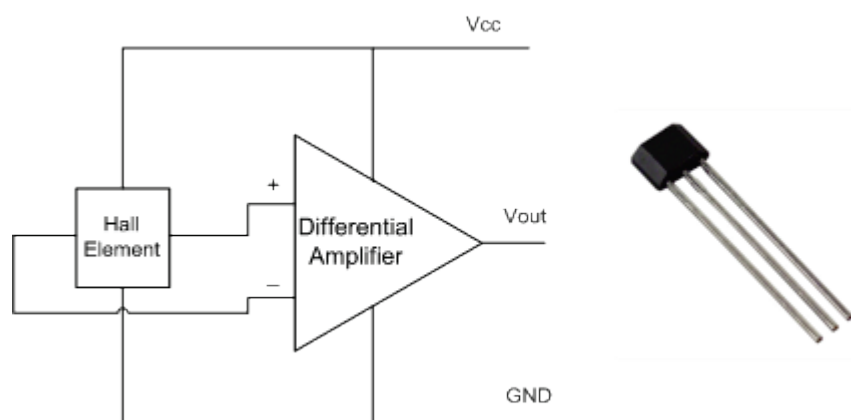
Fig. 3-5 Hall Effect Sensor Integrated Chip
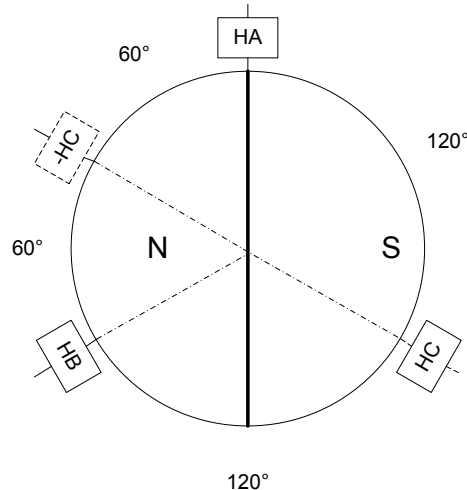
Fig. 3-6 Hall Placement for a Two Pole Motor

To illustrate the position sensing, a most simple rotor mode is used. This rotor only has two poles, a north pole and a south pole, and each of the poles takes up 180°. (Fig. 3-6) HA, HB and HC represent the positions of the Hall Effect sensors. The Hall Effect sensors are typically built inside the stator and do not rotate with the rotor. The Hall Effect sensor has either high or low output and the motor has six states when operating, so at least three Hall Effect sensors need to be implemented for distinguishing six different states. There are two ways to place the Hall Effect sensors. One is a 120° phase and the other is 60° phase. The motor designed is intended to use the first method.
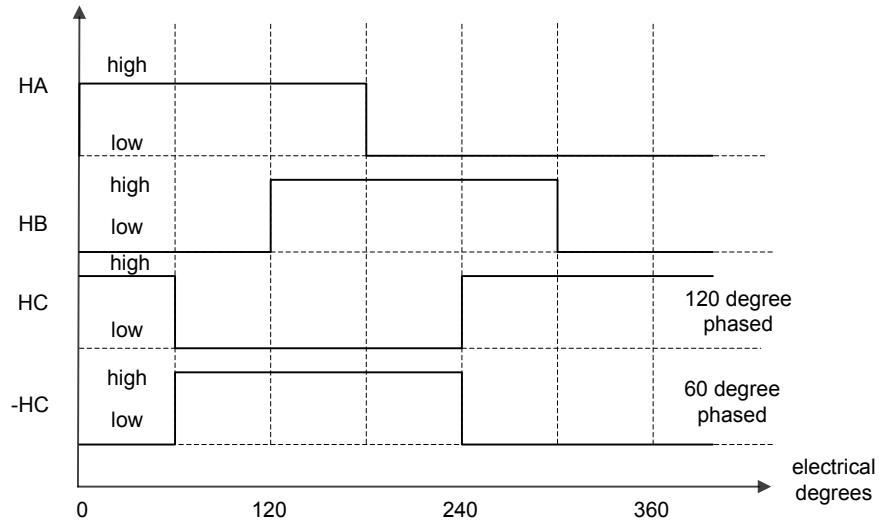
Fig. 3-7 Hall Outputs

When the rotor spins, the three Hall Effect sensors will generate three square waves that have a 120° difference in phase with each other in an electrical cycle (Fig. 3-7). In this simple case the number of electrical cycles will be exactly the same as mechanical cycles. For a rotor with more than two poles there is a relationship between Hall Effect sensor cycle (electrical cycle), Hall Effect sensor Frequency, mechanical cycle(motor spin revolution), motor speed and poles.

$$\frac{\text{Hall Effect sensor cycle}}{\text{Mechcanical cycle}} = \text{poles}\Big/2$$

$$\text{Motor Speed[RPM]} = \frac{\text{Hall Effect sensor frequency[Hz]*60}}{\text{poles}/2}$$

Table 3-1 shows the corresponded 120° phased Hall Effect sensor output and the input to the motor stator coils. As discussed in the previous section, the motor will be working in full-wave operation mode that for each state of the motor, a current is fed through two phases, leaving the third phase floating. The Hall Effect sensor states are

constrained in the first six states shown in the table and the bottom two states are invalid. If the Hall states jumped into these two states, there will be no input to the motor. This may happen under some conditions such as a Hall Effect sensor malfunction, noise problem, sensors position miscalculation, etc. It may cause motor to shut down since the motor has no input. Each of the first six states corresponds to a unique motor input. Based on the Hall Effect sensor outputs, the drive decides which switch to turn on, hence the specific phases will be fed with a current. As the Hall Effect sensor states repeat, the switch sequence (STEP1 to STEP7, refer to page 23) repeats for every electrical cycle.

Table 3-1 Hall States and Motor Input

120°			MOTOR		
HALL 1	HALL 2	HALL 3	A	B	C
1	0	0	H	X	L
1	1	0	X	H	L
0	1	0	L	H	X
0	1	1	L	X	H
0	0	1	X	L	H
1	0	1	H	L	X
1	1	1	X	X	X
0	0	0	X	X	X
1- HIGH LEVEL HALL SENSOR INPUT					
0- LOW LEVEL HALL SENSOR INPUT					
H- HIGH OR SWITCHING MOTOR OUTPUT					
L- LOW MOTOR OUTPUT					
X- MOTOR OUTPUT IS OFF (FLOATING)					

In one electrical cycle, the Hall Effect sensor outputs, Back EMF, Motor Phase inputs have a relation shown in Fig. 3-8. The back EMF is dependent on the shaping of the motor and the magnetic poles on the rotor. A proper design can achieve a trapezoidal

wave or a sinusoidal wave. No matter which wave shape the back EMF is, the way in which the servo amplifiers drive the motor stays the same, except that a slight difference of the torque output on the rotor may occur.
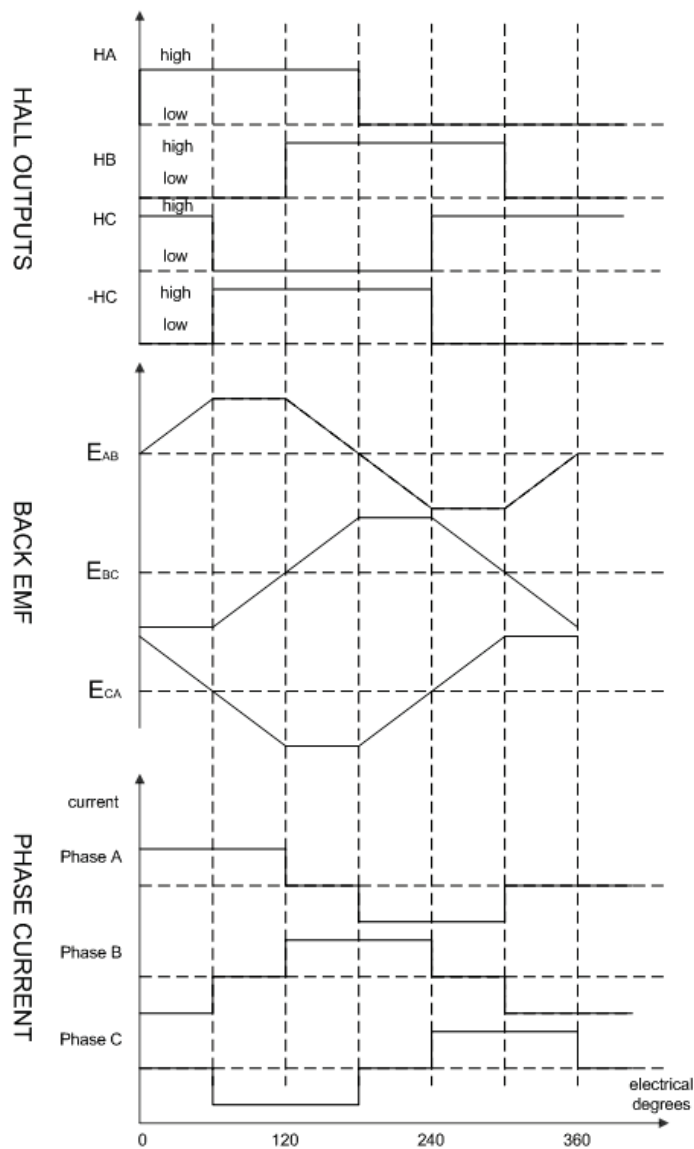
Fig. 3-8 Hall Outputs, Back EMF and Phase Current in One Electric Cycle

3.2.2   High Temperature Motor Hall Commutation

The principle of Hall commutation discussed in the previous section can be applied to the brushless DC motor, including the high temperature brushless DC motor designed previously.

The high temperature motor designed has four poles on the rotor and six poles on the stator. It is also intended to run at full-wave operation. According to the number of the magnetic poles on the rotor, there are two electrical cycles per mechanical revolution. Thus, the Hall states have two cycles in one mechanical cycle.

This typical design of poles allows to determine the positions of the Hall Effect sensor intuitively. The positions of the Hall Effect sensors are equally spaced around the rotor with an angle of 120° (Fig. 3-9). However, for other designs which have a different number of poles (ie. twelve poles on stator and eight poles on rotor), it requires calculation to position the Hall Effect sensor correctly. There may be multiple choices for the positions of the Hall Effect sensors, but the three Hall outputs must match the desired wave shapes (Fig. 3-7).
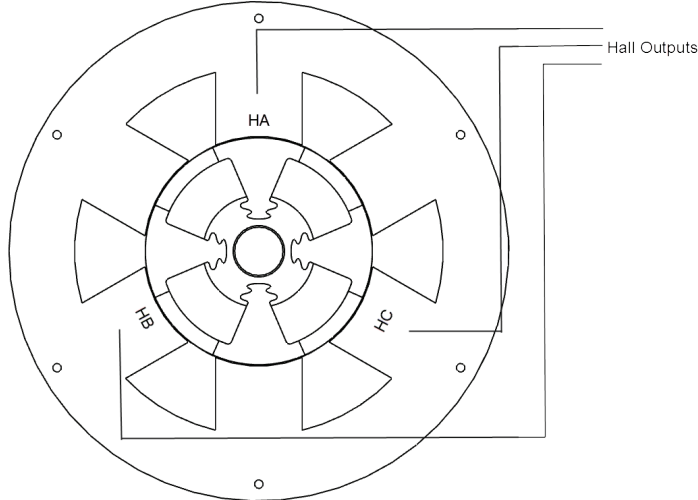
Fig. 3-9 Hall Effect Sensor Positions

The north poles and south poles are symmetrically distributed on the rotor. The following six figures (Fig. 3-10 through Fig. 3-15) describe the rotor position and its corresponding Hall states. For each of the figures, on the left side is the Hall outputs. The figure on the right side is the rotor position where the motor enters the state highlighted on the left side figure. The rotor rotates counterclockwise. For every 30° of rotation the Hall state changes. Meanwhile, the figure not only shows the rotor position, but also indicates the magnetic field that generated by the stator. As the rotor turns, the magnetic field alternates to apply a torque to accelerate the rotor.
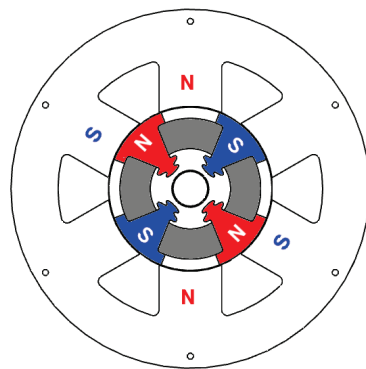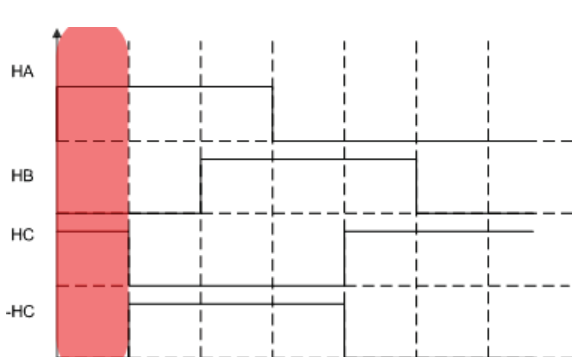
Fig. 3-10 State One
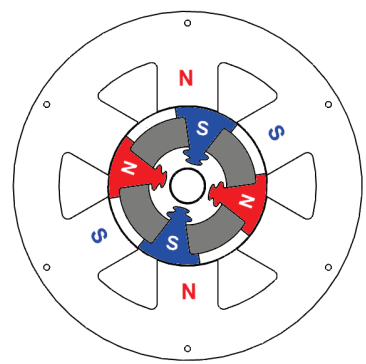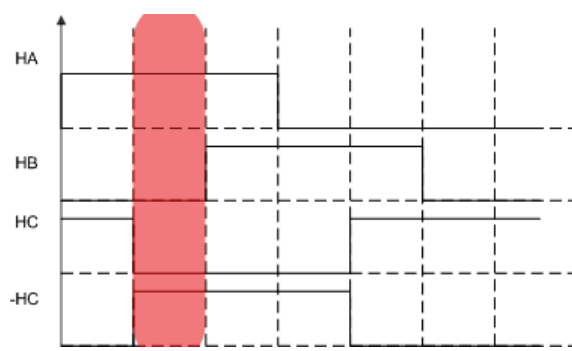
Fig. 3-11 State Two
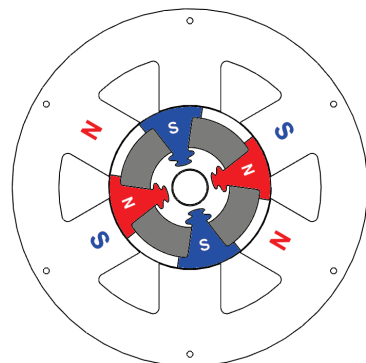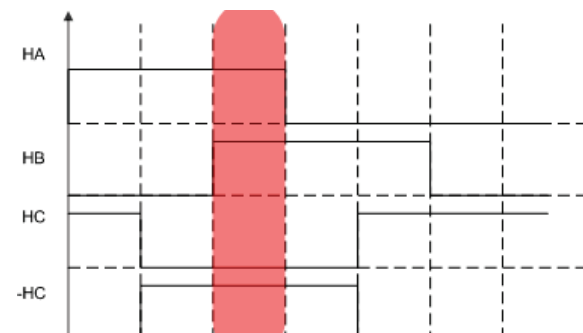
Fig. 3-12 State Three
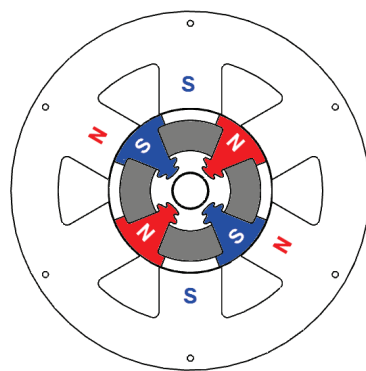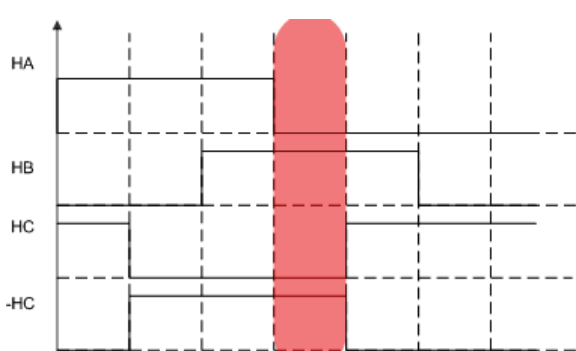
Fig. 3-13 State Four
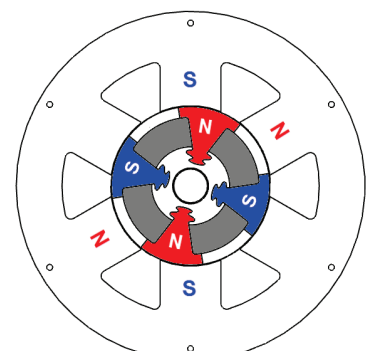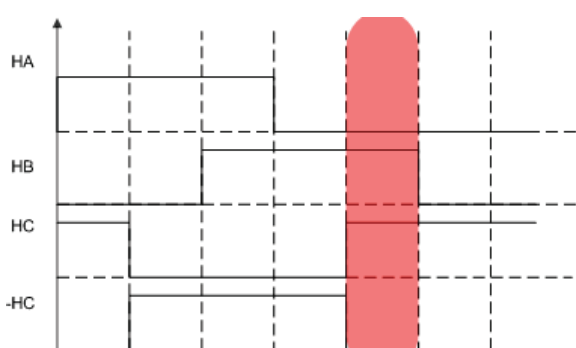
Fig. 3-14 State Five
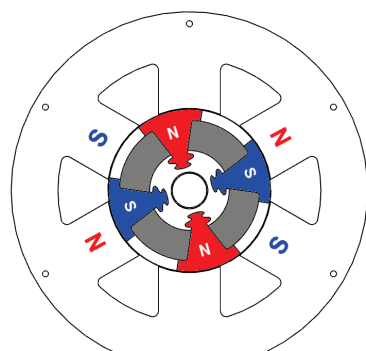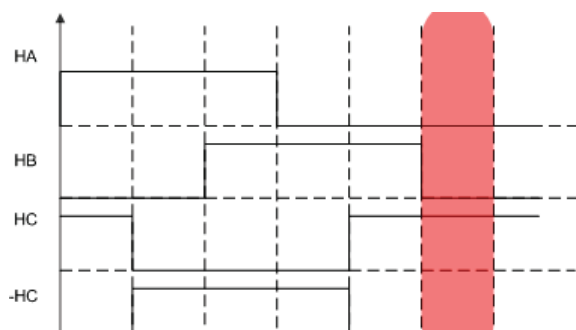
Fig. 3-15 State Six

3.2.3 Hall Effect Sensor Limitations in High Temperature Applications

Although the Hall state feedback is widely used in the brushless DC motors for rotor position sensing, temperature limits exclude the Hall Effect sensors from some applications. For the high temperature motor application, the Hall Effect sensors may not work properly when temperature is high. When temperature reaches the limit, the Hall sensors fail to work and, consequently, the switching logic will not know the position of the rotor. The motor will either be unstable or stop rotating.

Since the working principal of the Hall Effect sensor in a brushless DC motor is understood, an approach is developed to overcome the limitation which simulates the Hall states by using the high displacement sensor and the mechanical features of the rotor. The following section will discuss in detail how the Hall states are rebuilt using high temperature displacement sensors.

3.2.4 Generating Hall States by Using Displacement Sensor

The balancing holes are used to build the Hall states. On the rotor, there are two sets of equally spaced holes which are designed for balancing. In order to simulate the change of the Hall state, 12 cap screws are installed on one set of the balancing holes. For the other set of holes, two screws are put on at 180° interval, because there are two electric cycles per mechanical cycle.

Two high temperature displacement sensors are mounted on the side of the rotor, and detect the passage of the two sets of screws. The sensor output is calibrated such that

when facing the cap of the screw, the output is 0~1Volt; when facing the surface of the rotor, the output is 6 Volt. Hence, as the rotor spinning, two sets of periodical wave are generated. One is from the sensor detecting the set of 12 screws which has the frequency of 12 times the spin frequency. This signal is identified as "Clock". Meanwhile, the other sensor detecting the set of two screws generates a similar wave shape except that the frequency is one sixth lower. This signal is identified as "Reset". Fig. 3-16 shows the described set up of the displacement sensor and the screws around the rotor.
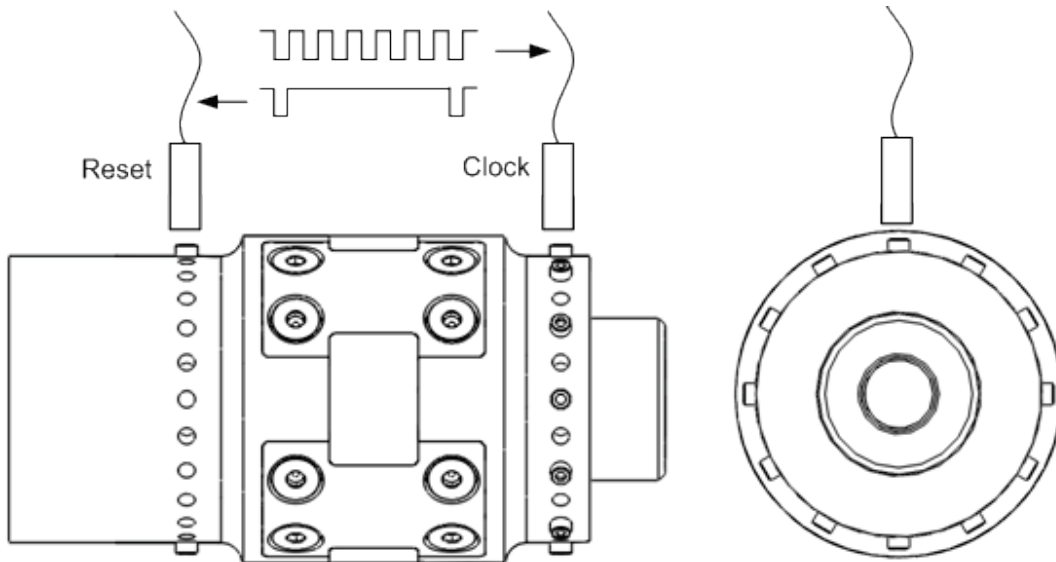
Fig. 3-16 Two Sets of Screws and High Temperature Displacement Sensors

The output from the displacement sensor is fed through a Schmitz trigger inverter, so that the two periodic waves are filtered into two clear square waves. The effect of the voltage unevenness due to the vibration of the motor is not observed from the filtered square waves. Since the position of the screws relates to the position of the magnetic

poles on the rotor, the information of rotor position is transmitted by these two square waves. The next take is to translate such implicit information into the known three Hall outputs(Fig. 3-17). Fig. 3-18 shows the screws on the motor spin rig.
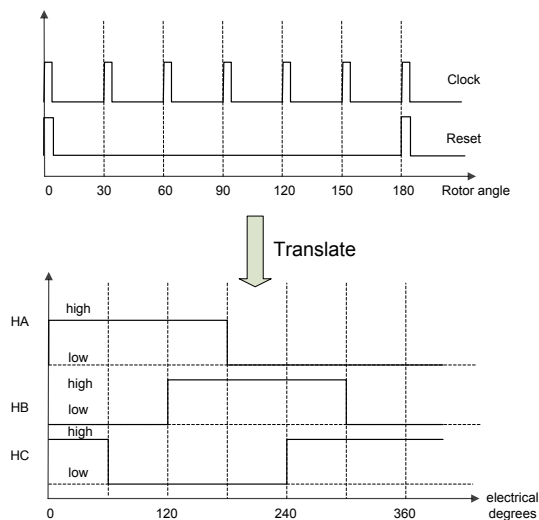
Fig. 3-17 Translating into Hall Output
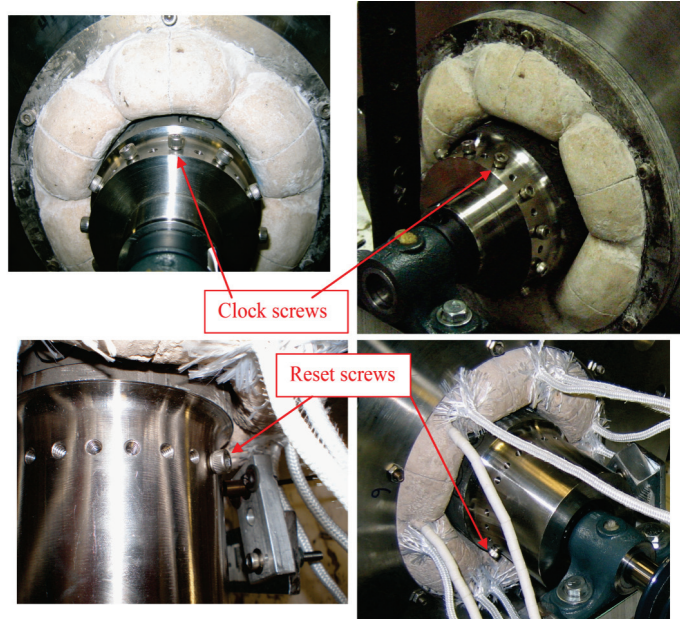
Fig. 3-18 Clock Screws and Reset Screws

3.2.5 Digital Circuit Design

A digital circuit is designed to accomplish the task of translation. As mentioned before, the positions of the screws are fixed with the positions of the magnetic poles. The displacement sensors identify the positions of the screws, hence a proper signal transformation identifies the position of the magnetic poles.

The relationship between rotor positions and the Hall states implies that a state change must occur every 30° of rotation. There are 12 screws around the rotor at the "Clock" that equally spaced with 30°, which is the same interval as the state change. Hence, if the sensor detects one passage of the screw, the Hall state changes to the next one. For a motor to operate at full-wave mode, six states are required for an electrical cycle. In a mechanical revolution, 12 changes of the states imply two electrical cycles. Once the sensor detects the passage of the screw on "Reset", one electrical cycle ends and another starts.

A sequential digital circuit is required to manipulate this digital signal. To make this design simple, a 4-bit binary counter with several logic gates are utilized. The signal from the displacement sensor detecting the 12-screw side is connected to the CLK port of the counter and the signal from the other displacement sensor is wired to the RST (LD) port of the counter. This is the source of the "Clock" and "Reset" names.

Here are the design details of the logic circuit. First, the State Table (Table 3-2) is formed. The last six states of the counter are used to form three intended Hall outputs (HA, HB, HC). A Karnaugh map (K-Map) approach is used to simplify the boolean algebra expressions (Table 3-3, Table 3-4, Table 3-5).

Table 3-2 State Table

Q$_D$	Q$_C$	Q$_B$	Q$_A$	HA	HB	HC
1	0	1	0	1	0	1
1	0	1	1	1	0	0
1	1	0	0	1	1	0
1	1	0	1	0	1	0
1	1	1	0	0	1	1
1	1	1	1	0	0	1

Table 3-3 K-Map for HA

		Q$_C$	
Q$_B$	Q$_A$	0	1
0	0	X	1
0	1	X	0
1	1	1	0
1	0	1	0

Table 3-4 K-Map For HB

		Q$_C$	
Q$_B$	Q$_A$	0	1
0	0	X	0
0	1	X	0
1	1	0	1
1	0	1	1

Table 3-5 K-Map for HC

		Q$_C$	
Q$_B$	Q$_A$	0	1
0	0	X	1
0	1	X	1
1	1	0	0
1	0	0	1

From the K-Map simplification, the final expressions for the three Hall outputs are

found,

$$HA = \bar{Q}_C + \bar{Q}_B\bar{Q}_A$$

$$HB = \bar{Q}_B + Q_C\bar{Q}_A$$

$$HC = Q_B(\bar{Q}_A + Q_C)$$

A scheme of the digital circuit is sketched in Fig. 3-19.
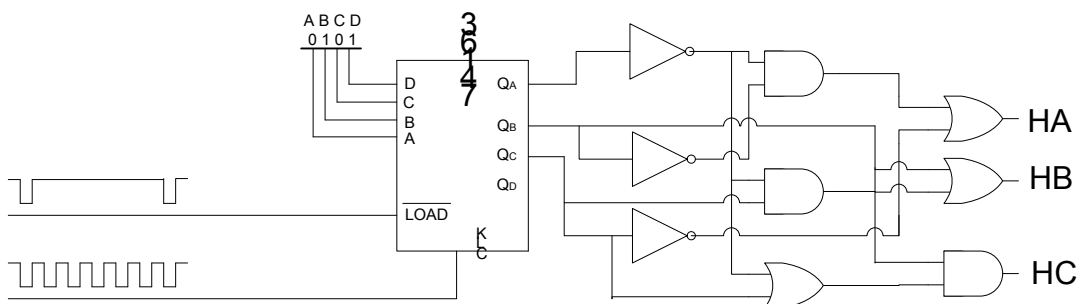
Fig. 3-19 Scheme of the Digital Circuit

As each screw passes the displacement sensor, the counter adds up one, leading the Hall state to shift to the next one. After six "Clock" pulses, a "Reset" pulse resets the Hall state to the first one. The reset prevents error from accumulating. Otherwise, during the operation, there might be a miscount or overcount due to noise or some other reason. If a miscount occurs, the position information created by the digital circuit is 30° lag from the actual position of the rotor. Because of the existence of "Reset", this lag will last for at most a half revolution. The digital circuit resets when a "Reset" pulse comes, the position lag will not be brought to the next half revolution.

3.2.6　Digital Circuit Implementation

　　The CMOS logic chips from 74HC series is chosen to implement the logical circuit. Table 3-6 lists the integrated chips required for this logic circuit. They are inexpensive, yet have fast response. The digital circuit is implemented on a bread board (Fig. 3-20) and the designed function is fully tested.

Table 3-6 List of IC for Logic Circuit

Quantity	Description	Serial Number
1	IC QUAD 2-INPUT AND GATE 14-DIP	SN74HC08N
1	IC HEX INVERTER 14-DIP	SN74HC04N
1	IC QUAD 2-INPUT OR GATE 14-DIP	SN74HC32N
1	IC 4-BIT BINARY COUNTER 16-DIP	SN74HC163N
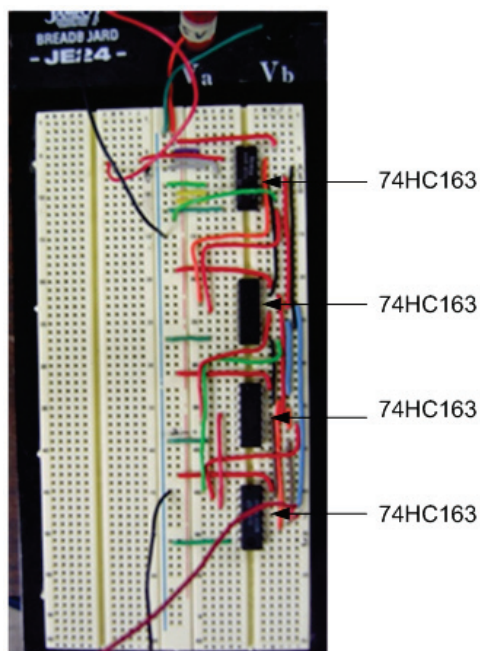
Fig. 3-20 Implementation of Digital Circuit
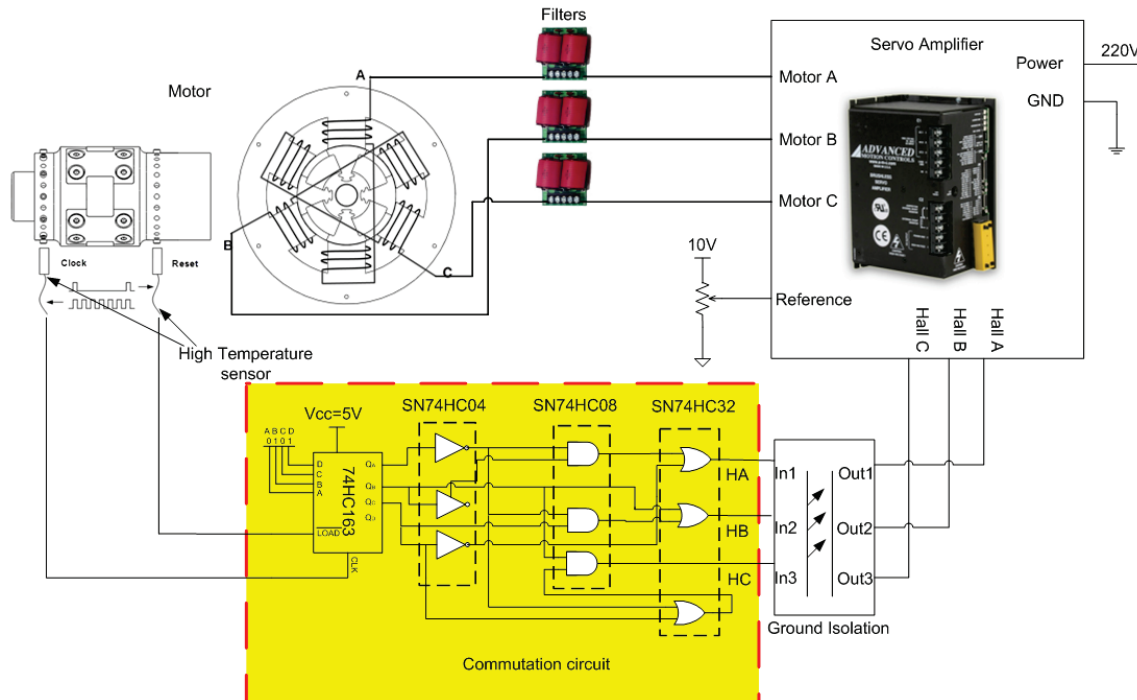
Fig. 3-21 Digital Commutation Circuit in Feedback Loop

Fig. 3-21 shows the complete motor drive circuit. The highlighted area is the digital circuit for commutation. More details of the complete drive circuit are discussed in the next section.

3.2.7 Verification of the Digital Circuit

Initially, a function generator is used to simulate the "Clock" and the "Reset" signals that are received from the high temperature probes. A square wave, the "Clock", is generated by the function generator and another square wave whose frequency is one sixth of the Clock's is inputted as the "Reset". The circuit is validated. In the left corner of Fig. 3-22, the screen shot of the oscilloscope shows the "Clock" and one of the simulated

Hall outputs.

With the implementation of circuit verified as correct, the circuit is tested by using the motor spin test rig. An auxiliary motor is used to drive the rotor with a pulley and belt mechanism (Fig. 3-23). Meanwhile, the high temperature sensors are mounted to detect the passages of screws (Fig. 3-24). The rotor is spinning at approximately 2500 rpm. The result shows that the three Hall states are successfully generated by using the outputs from the high temperature displacement sensors (Fig. 3-25).

Fig. 3-22 Test of Digital Circuit Using Function Generator
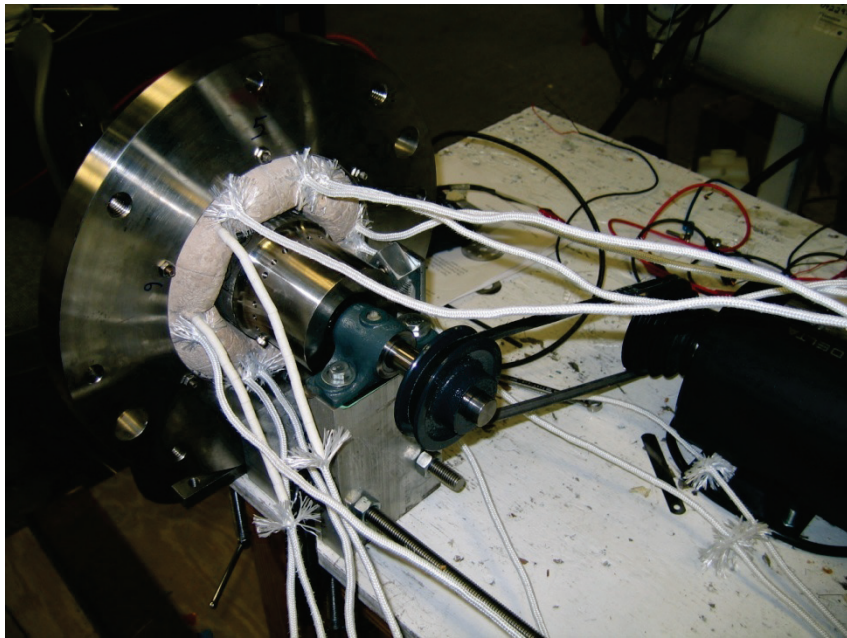
Fig. 3-23 Motor Driven by Auxiliary Motor
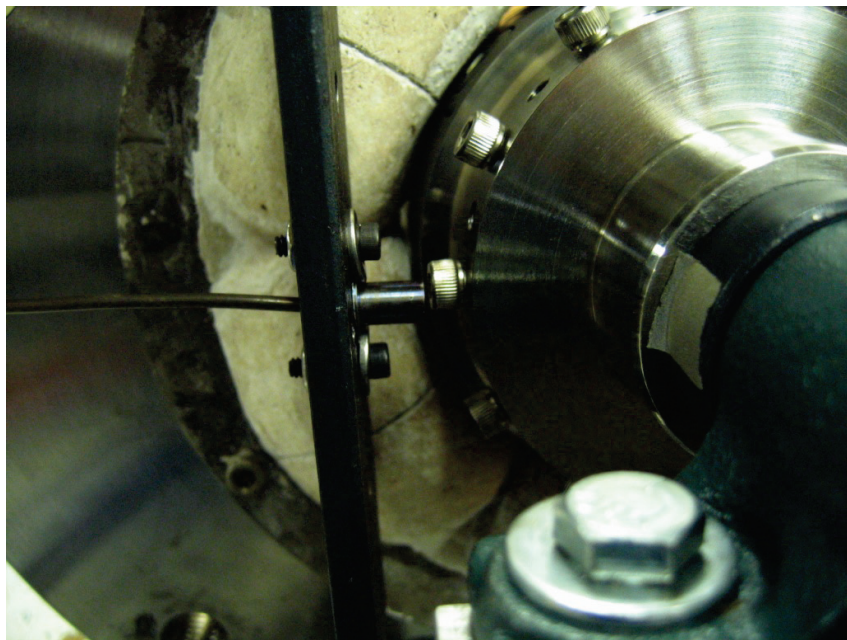
Fig. 3-24 High Temperature Displacement Sensor Detecting Screws

Fig. 3-25 Two of the Hall Outputs (HA, HB)

3.3   Motor Drive

There are several ways to drive the permanent magnet brushless DC motor. Most of these methods use rotor position feedback to control the motor. One exception is to use a sensorless approach which detects the back EMF in an unexcited phase to determine the commutation point.

In this section, various ways of motion control for a brushless DC motor are introduced, and the method for driving the high temperature motor is selected.

3.3.1   Methods of Motion Control

- Servo Amplifiers

Servo amplifiers are used in motion control to achieve precise control of position and velocity. The amplifier translates low energy reference signals to high energy signals. It usually has the capability to use multiple types of position information from Hall Effect sensors, encoders and tachometers. The IGBT drive, PWM module, switching logic, filters are built together. AMC(Advanced Motion Control) has a wide variety of servo amplifiers available. Fig. 3-26 shows the block diagram of the servo amplifier approach.
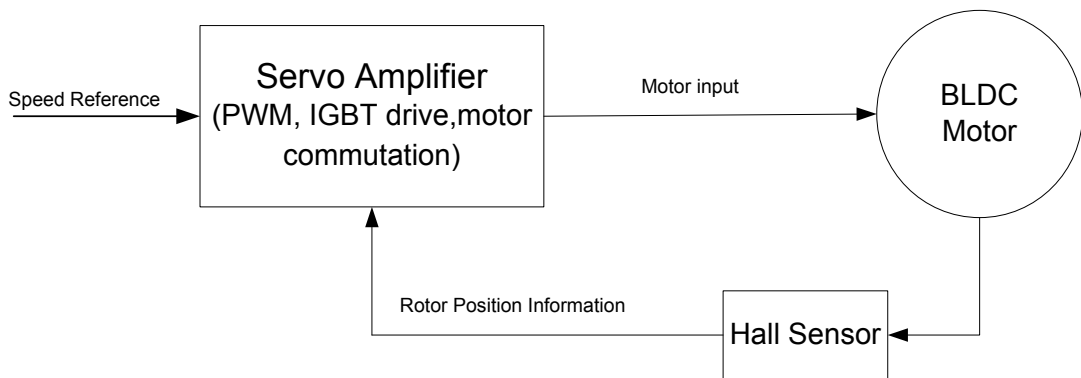
Fig. 3-26 Scheme of Servo Amplifier for Motion Control

- Microcontrollers

Microcontrollers are used for low cost applications. A single chip can handle all of the signal processing, logic switching, PWM signal generating and motor commutation to perform simple speed control.

- Digital Signal Processor (DSP)

A DSP provides high speed, high resolution motor control. It allows to implement

control algorithms for a sophisticated motion control. It can handle a multivariable system, use neural networks and fuzzy logic, implement filters, perform a diagnostic monitor, etc. Sensorless approach relies on the high speed calculation of DSPs. The block diagram is shown in Fig. 3-27.
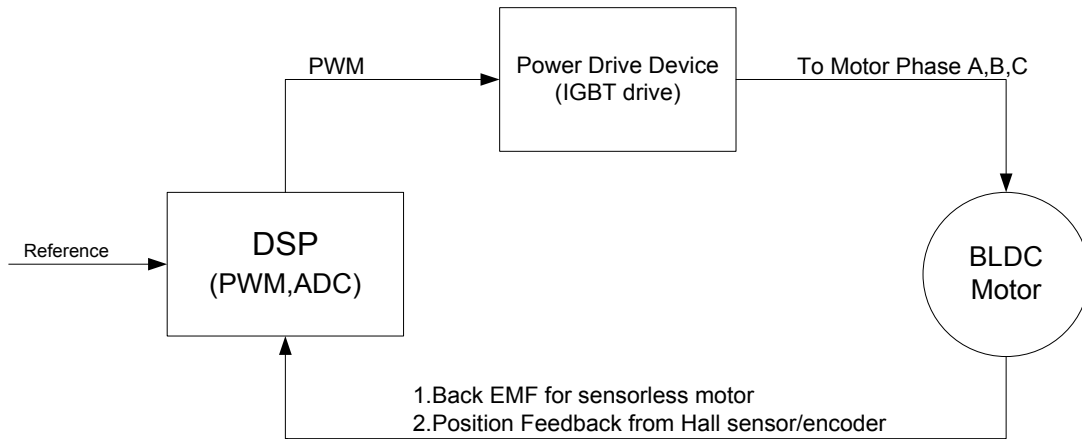
Fig. 3-27 Scheme of DSP for Motion Control

3.3.2   Motion Control Plan of High Temperature Motor

Depending on the resources and the requirements of the motor, a servo amplifier is chosen for the motion control. Here, an AMC analog servo amplifier mode B30A40AC is selected. Fig. 3-28 shows the appearance of the B30A40AC servo amplifier and Fig. 3-29 shows the circuit of the servo amplifier [5]. A more detailed discussion for the motion control of the high temperature motor is in the next section.

Fig. 3-28 AMC B30A40AC Servo Amplifier

Fig. 3-29 Block Diagram of the Servo Amplifier
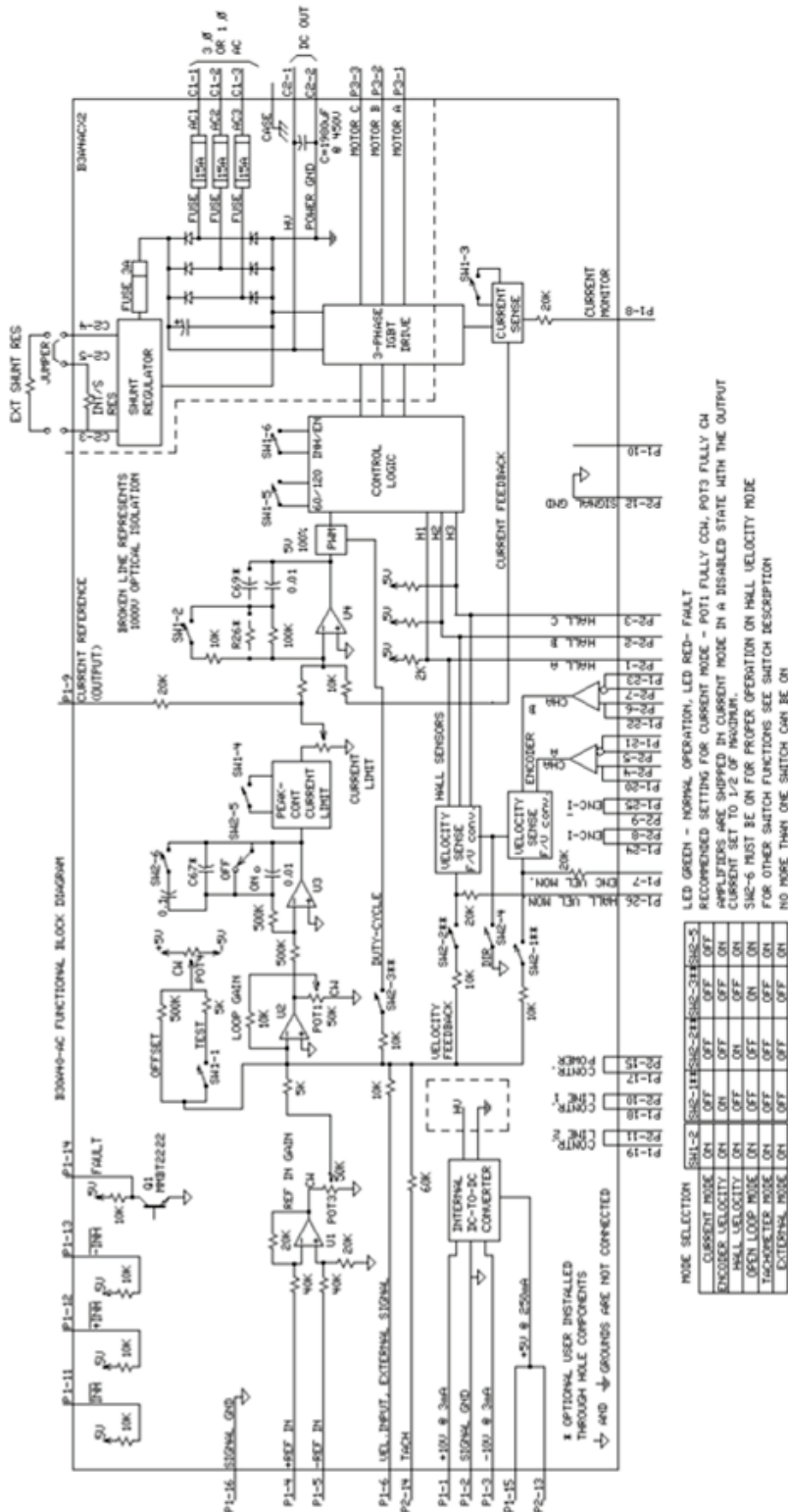
4. MEASUREMENT AND TEST

In this section, several measurements are shown and the results of these measurements define the characteristics of the motor. Motor spinning is demonstrated at room temperature on the motor test rig.

4.1 Motor Stator High Potential Test

The reliability of the motor at high temperature depends on the coils of the motor. It is known that poor winding or unsuccessful potting may break down the coils when fed with high voltage at high temperature. The high potting test is used to check the break down voltage and the equivalent resistance between each individual coil and laminated stator at both room and high temperature. This is a necessary process to verify that the high temperature coils will not fail at the extreme environment. All high temperature components (high temperature magnetic bearing, high temperature thrust bearing) must survive the high potential test before they can be used for high temperature applications.

Fig. 4-1 Motor Stator in Oven for High Potential Test

First, high potential test is conducted first at room temperature. By applying 500V AC or DC between the stator and one of the coils, the current is measured. The test is repeated for all six coils to complete the room temperature high potential test. For the high temperature high potential test, it is shown in Fig. 4-1 and Fig. 4-2 that the stator of the motor is put into an oven and heated to 1000°F. Again, 500V AC or DC is applied between the stator and each coil.

Table 4-1 shows measurements of the current with 500V applied between the stator laminates stack and an individual coil. The results appear excellent even at 1000°F. The stator is proven to work since the actual maximum operating voltage will not exceed 240V.
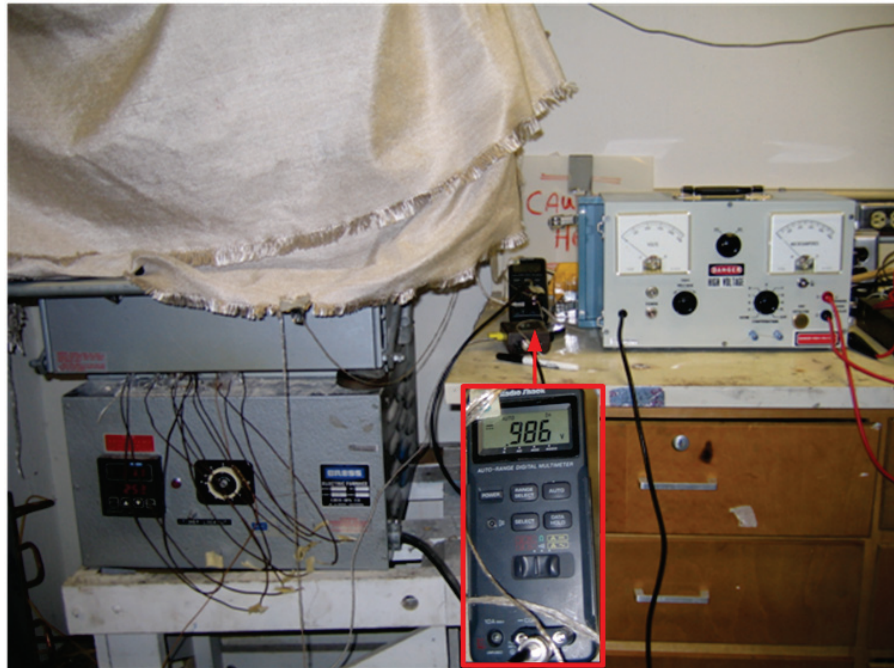
Fig. 4-2 Heat up to about 1000°F

Table 4-1 Stator High Potential Test Result

| Pole | Input Type | 1000°F | | | 75°F | | |
		Voltage (V)	Current (µA)	Equivalent Resistant (MΩ)	Voltage (V)	Current (µA)	Equivalent Resistant (MΩ)
1	DC	500	100	5.000	500	10	50.000
	AC	500	260	1.923	500	30	16.667
2	DC	500	100	5.000	500	10	50.000
	AC	500	260	1.923	500	30	16.667
3	DC	500	100	5.000	500	10	50.000
	AC	500	240	2.083	500	30	16.667
4	DC	500	140	3.571	500	10	50.000
	AC	500	350	1.429	500	30	16.667
5	DC	500	160	3.125	500	10	50.000
	AC	500	380	1.316	500	30	16.667
6	DC	500	160	3.125	500	10	50.000
	AC	500	540	0.926	500	80	6.250

No sign of breakdown appears during the entire high potential test. It is found that

AC source tends to apply more current than DC source. A significant increase in current from the room temperature to 1000°F is noticed. This verifies that high potting must be performed at high temperature in order to check the integrity of the insulation at high temperature.

Fig. 4-3 shows the stator after the high potential test. The extended part of the high temperature wire appears fluffy. This appearance is due to the fiber coating for insulating the wires becomes loose and separates from the wires at high temperature. Yet, inside the coils, there is no problem since the fiber is constrained. But, the loss of fiber coating at the non-coil part will leave the wire exposed. Long high temperature sleeves are used for protecting that part of the wires (Fig. 4-4).
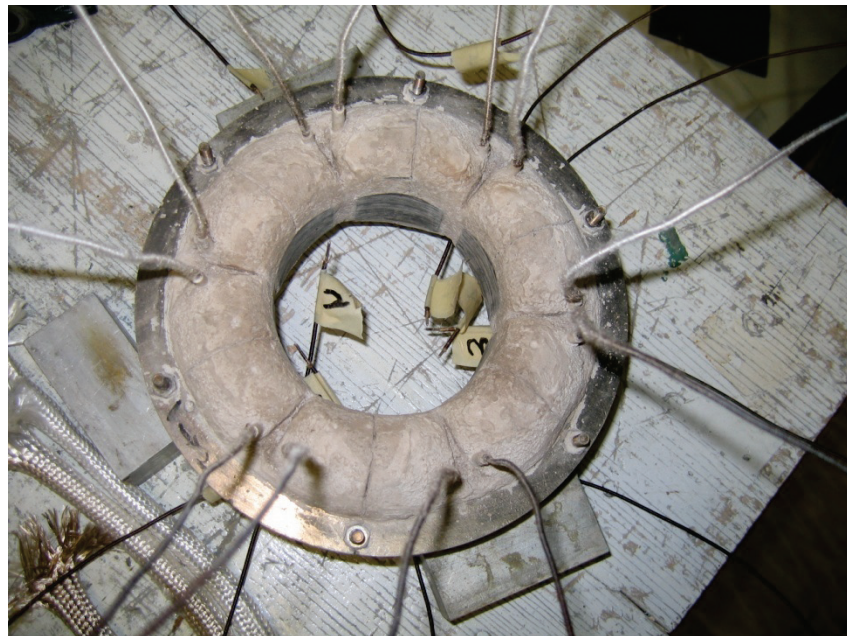
Fig. 4-3 Stator after High Potential Test
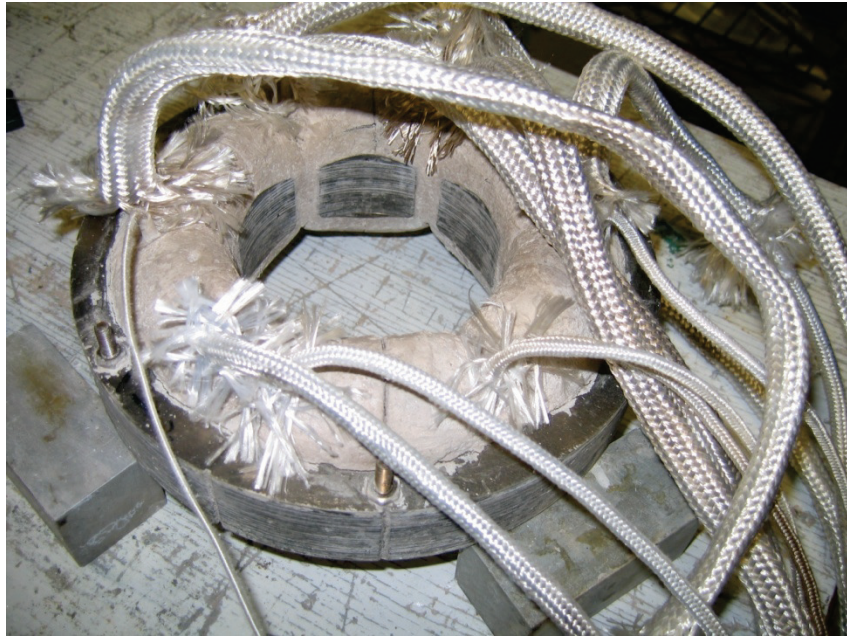
Fig. 4-4 Sleeves for Protecting the Wires

4.2   Coil Inductance, Resistance and Capacitance Measurement

The motor servo amplifier has a minimum inductance requirement for the coil of the motor. Because the amplifier uses PWM, low inductance allows the high switching noise to be inputted into the motor phase, which may lead to motor malfunction. The inductance, capacitance and resistance of one coil are measured at 120 and 1000 Hz. The measured results are shown in Table 4-2. Due to the similarity of the coils, only one is measured.

The inductance of the motor phase is dependent on the rotor angle and frequency. The higher the frequency is for the motor, the lower the inductance is. The minimum requirement during operation for the AMC B30A40AC servo amplifier is 600μH. The measurement shows the coil inductance is too low to meet the requirement. Extra

inductance must be added for each phase. AMC provides a type of filter to smooth the PWM output by adding extra inductance. Three AMC FC15030 filters are connected in series with the servo drive output which result in an extra 150µH inductance for each phase. Fig. 4-5 shows that there are three AMC filters connected.

Table 4-2 Measurement of Inductance, Resistance and Capacitance

Rotor Angle	Inductance at 120Hz (µH)	Resistance at 120Hz (Ohm)	Capacitance at 120Hz (µF)	Inductance at 1000Hz (µH)	Resistance at 1000Hz (Ohm)	Capacitance at 1000Hz (µF)
0	504	0.85	2330	368	7.9	61
15	520	0.88	2300	388	8.3	58
30	504	0.88	2490	419	10.5	56
45	516	0.87	2260	386	7.8	57.5
60	466	0.73	2020	465	6	64
75	431	0.66	1780	300	5.5	71.7
90	478	0.73	1880	478	6.9	63
105	516	0.8	1790	384	7.5	57
120	504	0.79	2000	503	9.5	54
135	522	0.8	1730	392	7.4	55
150	487	0.76	1520	357	7	61
165	432	0.67	1540	300	5.2	70
180	478	0.75	1540	348	6.5	62
195	527	0.81	1590	389	7.2	55.4
210	525	0.81	1760	434	9.4	52
225	541	0.83	1660	392	7.3	55
240	501	0.77	1700	360	6.8	60
255	432	0.68	1660	297	5.3	71.3
270	501	0.77	1770	362	7	60.4
285	537	0.83	1750	389	7.4	56
300	522	0.81	1900	425	9.5	53
315	528	0.81	1810	394	7.8	56
330	478	0.74	1850	347	6.9	63
345	431	0.67	1680	398	5.4	72
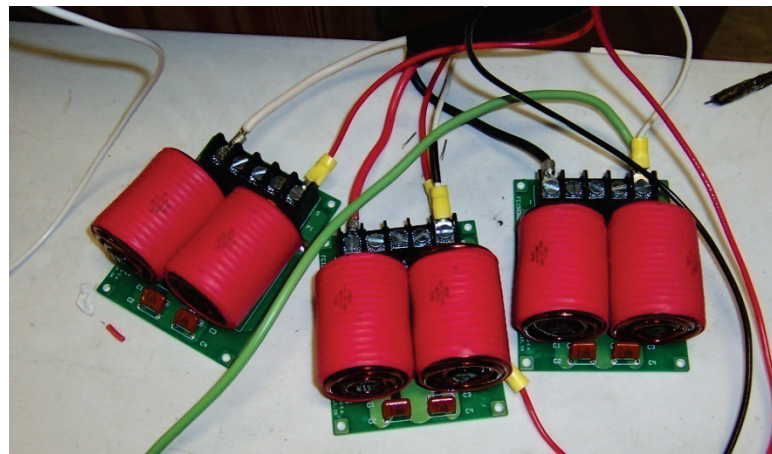
Fig. 4-5 FC13030 Filters

4.3   Static Torque Measurement

In the previous motor design discussion, the result shows that the output torque of the high temperature motor depends on current only. Torque output from the motor is proportional to the current that is conducted in the motor phase. A measurement is performed to find torque versus phase current. At each motor operation state, current is conducting in two phases only, and the third phase floats. By feeding current from phase A to Phase B with a DC voltage and allowing phase C to float, the motor is set to a motor operation state (Fig. 4-6). Fig. 4-7 shows how the DC source is connected to the motor phases. The current direction is also marked for this motor state

.
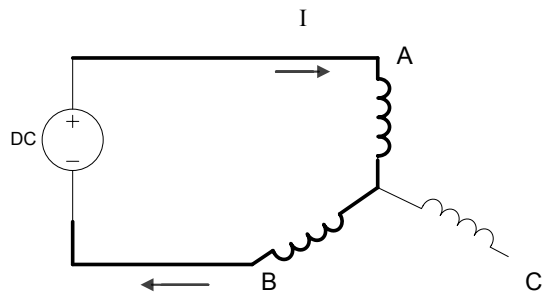
**Fig. 4-6 Scheme for Current Input**
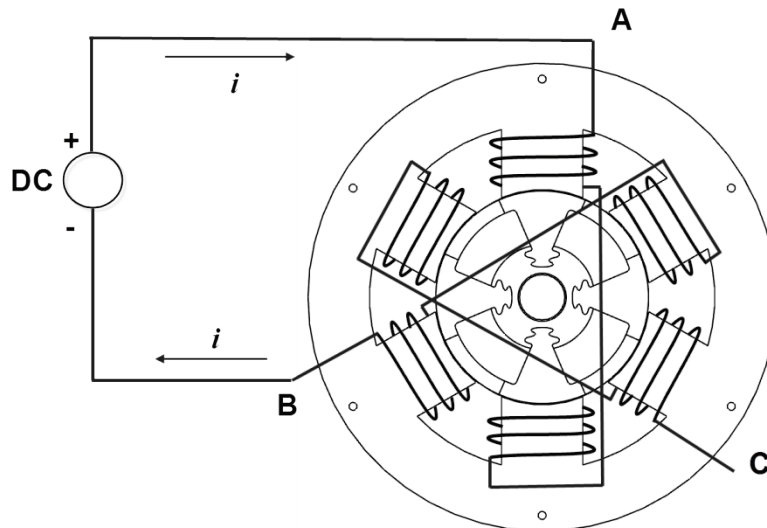
Fig. 4-7 Current Input for Torque Measurement

The method to measure the torque is sketched in Fig. 4-8. A string is attached to the pulley which is fixed with the rotor. The other end of the string is tied to a force gauge that can measure the tension of the string. The force gauge is clamped on a vise, which can move slowly in the direction of the string. The frictional forces at the bearings and the roller are ignored. The rotor is assumed to be at equilibrium as the force gauge moves slowly enough. The force transmitted to the string is equal to the tangential force acting on the pulley. The force gauge measures the tangential force. Hence, the output torque from the motor is found by knowing the force and pulley radius.

Since only two phases are excited, the static torque output varies with the position of the rotor. Maximum torque points exist. Because the four poles on the rotor are symmetric, the static force should repeat at every 180°. Thus, there are two maximum torque points separated by 180° in rotor position. Ideally, the values of the torque at these two maximum points are the same and they are proportional to the current. By moving

the force gauge slowly along the force direction, the maximum torque points are located as well as the maximum torque.
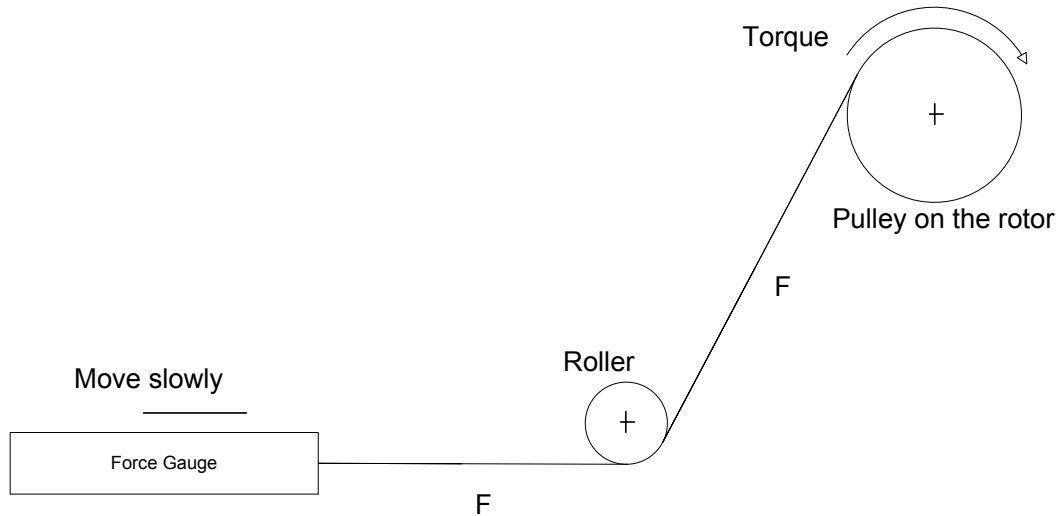
Fig. 4-8 Scheme of Torque Measurement

Fig. 4-9 shows the pulley fixed on the rotor and the roller mounted on the table. The string used to transmit the force is attached to the pulley. Fig. 4-10 shows the force gauge clamped on a vise, which is clamped to the fixed table. The force gauge is constrained to one translational degree of freedom such that it may only move along the direction of the string. Moving the force gauge slowly as the rotor completes one revolution allows two maximum points to be found.
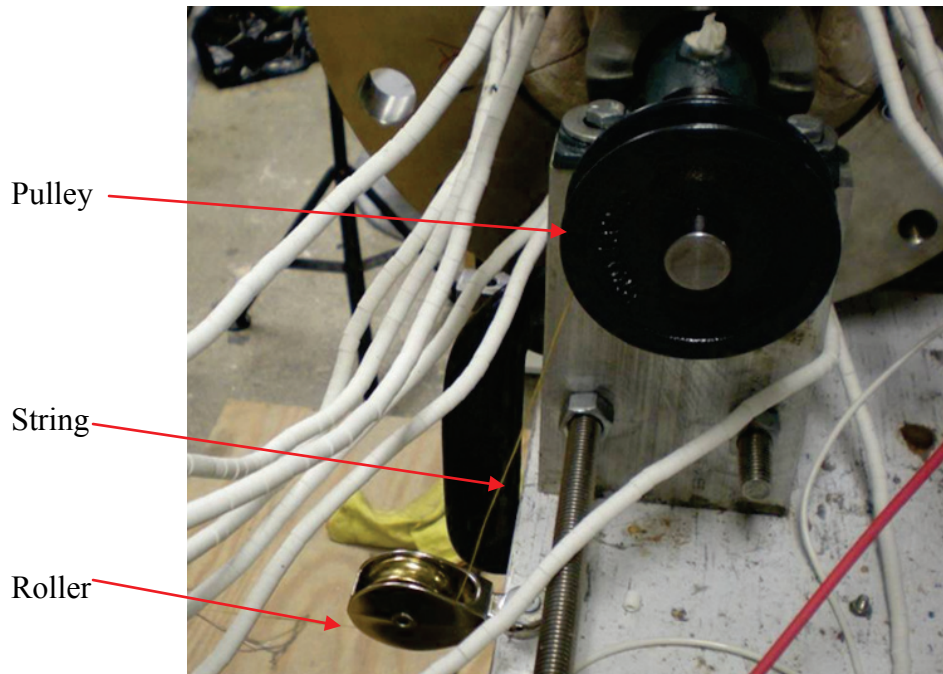
Fig. 4-9 String Attached to the Pulley
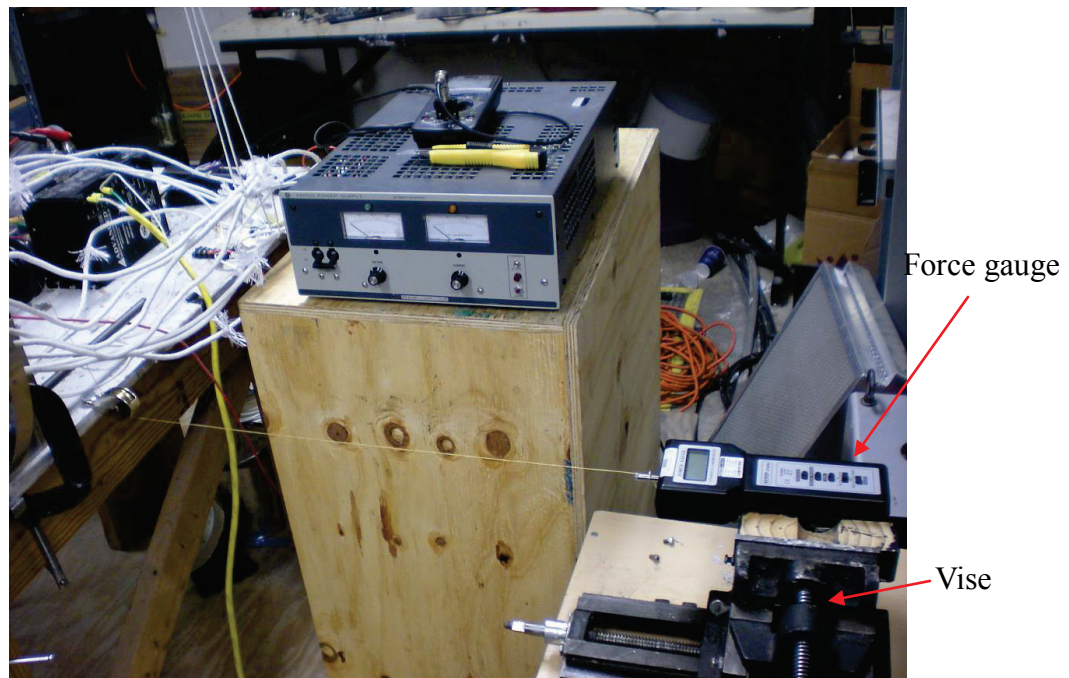
Fig. 4-10 Force Gauge for Measuring the Torque
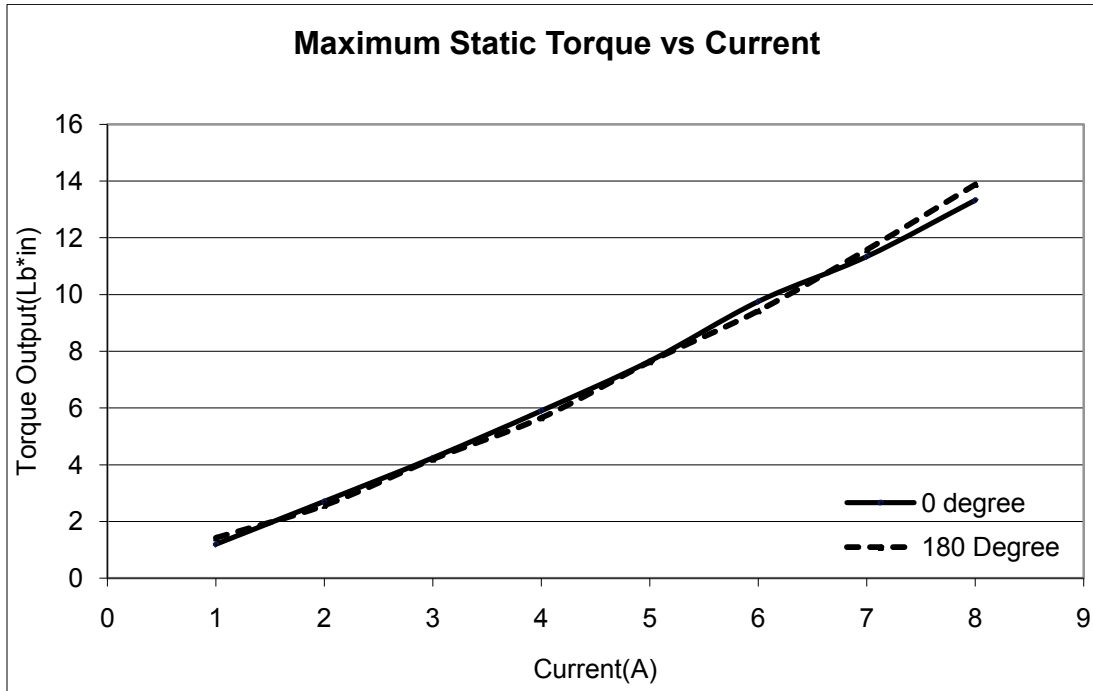
Fig. 4-11 Maximum Torque Versus Current

The process is repeated with different current levels. The relationship between the maximum torque and current is shown in Fig. 4-11. The solid line represents the first maximum point while the dashed line represents the second maximum point, which should be 180° from the first point. It is shown that the maximum torque is approximately 14 pound inch (1.58 Newton meter) with a constant current of eight Amps. The figure verifies that two maximum torques in each revolution are very close to each other, which is implied by the symmetry of the rotor. The maximum torque is proportional to the current. The linearity of the torque-current curve is acceptable.

The maximum torque may be used to predict the power output of the motor. The designed power output is 5.1kw with 10A current input with a motor spin speed at 20000 rpm. The actual power output predicted by using the measured static torque is calculated

as

$$P = T_m \cdot \omega = 1.58 \cdot 20000 \cdot 2\pi / 60 / 80\% = 4.2 kw$$

The designed 5.1kw power output is predicted by the FEM model which is the ideal value. There are many factors that cause power loss. The measured torque output may not consider the effect of frictional forces and winding loss. Yet, the results show that the motor built approximates the intended design.

4.4 Room Temperature Spin Test

The ultimate goal of building the motor test rig is to make the motor spin and achieve self-starting capability. As mentioned, the motion control will be handled with the AMC analog servo amplifier. In the previous sections the principal of the Hall Effect sensor, and how it senses the position of the rotor, are discussed. Then, the way to use two high temperature displacement sensors to create equivalent three Hall outputs is illustrated. The simulated Hall feedback signals to the servo amplifier accomplish closed loop motion control.

4.4.1 Closed Loop Operation

Fig. 4-12 shows the closed loop circuit of motion control using the servo amplifier. Three filter cards are used to add extra inductance for three phases. In the closed loop motor drive circuit, rotor position is obtained by using the high temperature sensor

detecting the passages of the screws. The digital circuit translates such outputs into three Hall outputs, which are then fed back to the servo amplifier. Reference signal with the range of 0 to 10 V provides the command of the motor speed.
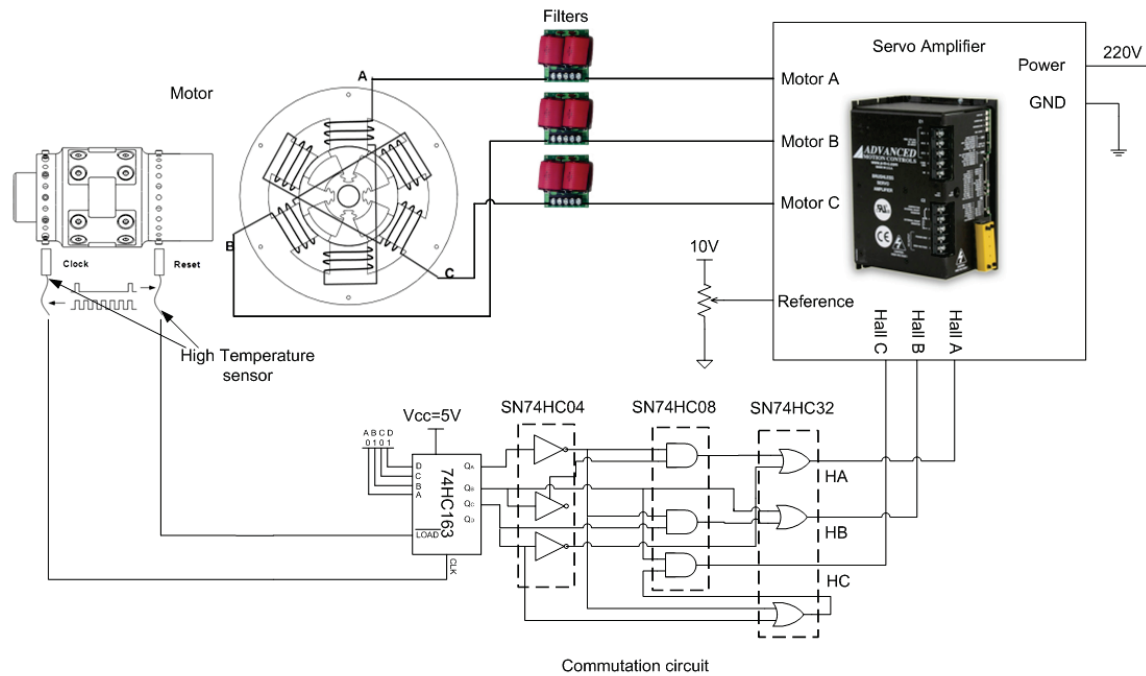
Fig. 4-12 Closed Loop Circuit

Fig. 4-13 shows the motor test rig including high temperature sensors, digital circuit, high temperature motor, servo amplifier auxiliary motor, etc.
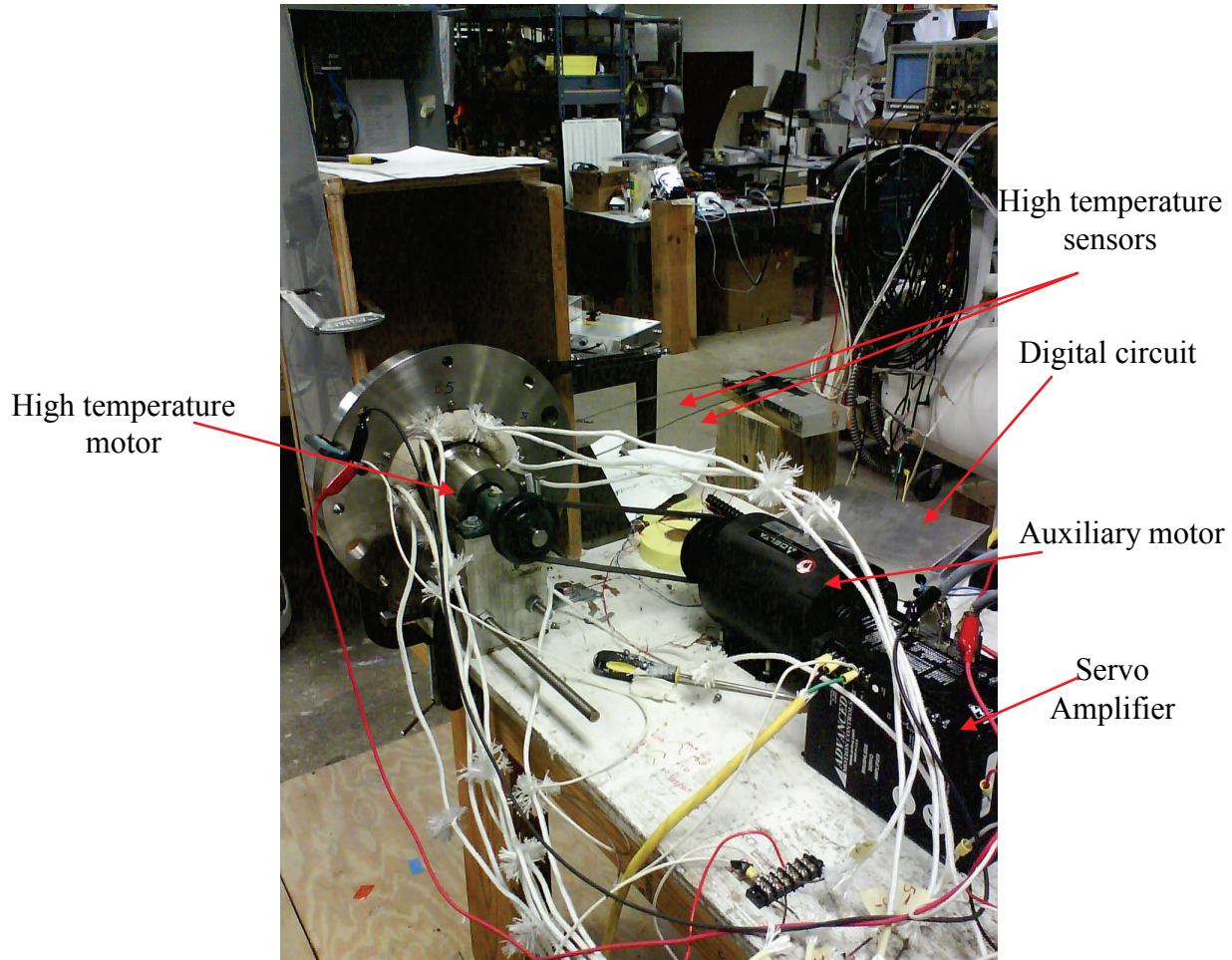
Fig. 4-13 Closed Loop Test Rig

4.4.2   Ground Loop Problem

Problems are found when the servo amplifier is activated. The servo amplifier gives an error that the voltage levels of the Hall feedback are boosted. The levels are no longer in the logic signal range of 0-5 Volts. Inspection shows the problem originates from the ground loop. The servo amplifier and digital circuit are co-grounded. Because of this ground loop, the outputs of the digital circuit have the addition of a constant voltage

which makes the system quit.

A ground isolation amplifier is used to separate the ground of servo amplifier and that of the digital circuit (Fig. 4-14). The ground isolation amplifier has an amplification factor of one, so it will not change the voltage level of the Hall signal, but will terminate the ground loop. In magnetic bearing control loops, the ground isolation is commonly used.
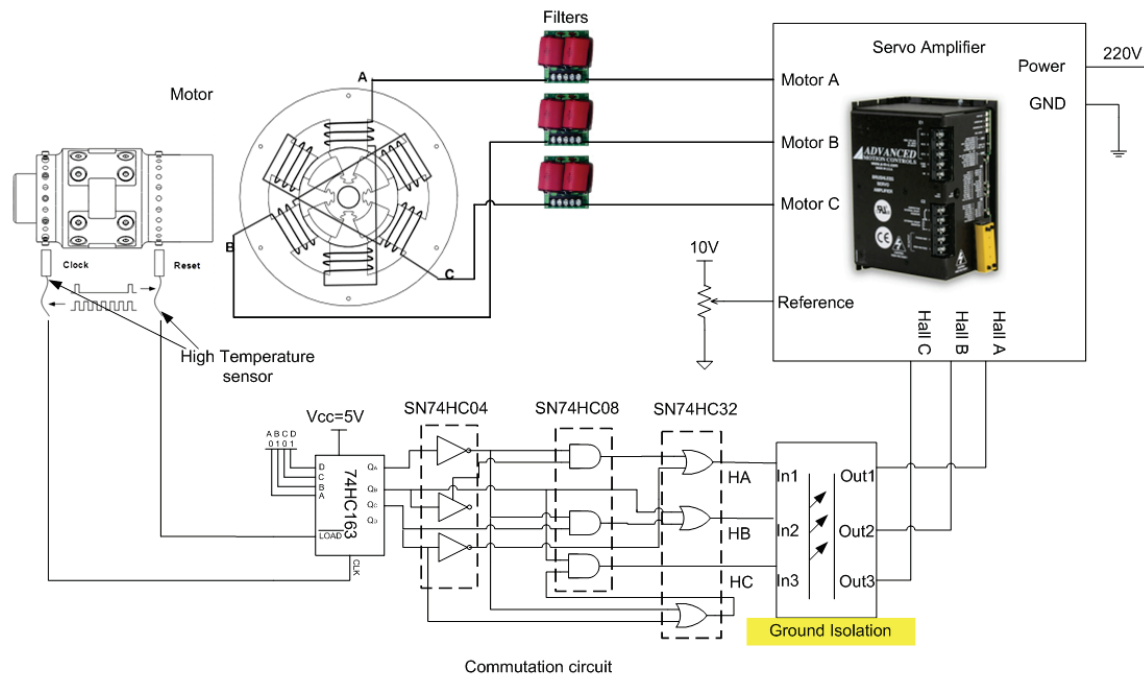

Fig. 4-14 Closed Loop with Ground Isolation

At first, the ground loop is considered the only problem that causes the servo amplifier to not be able to receive the rotor position feedback. However, other problems are present.

4.4.3 Noise Problem

Although the servo amplifier does not indicate any errors, the motor starts to move randomly once the drive is activated. It appears the closed loop circuit is suffering from a noise problem. The following test is performed to determine the major sources of the noise.

To confirm the problem is not caused by the PWM high switching frequency from the servo amplifier, the servo amplifier outputs are disconnected from the motor phases. Then, the rotor is driven by the auxiliary motor at 2500 rpm (Fig. 4-15).
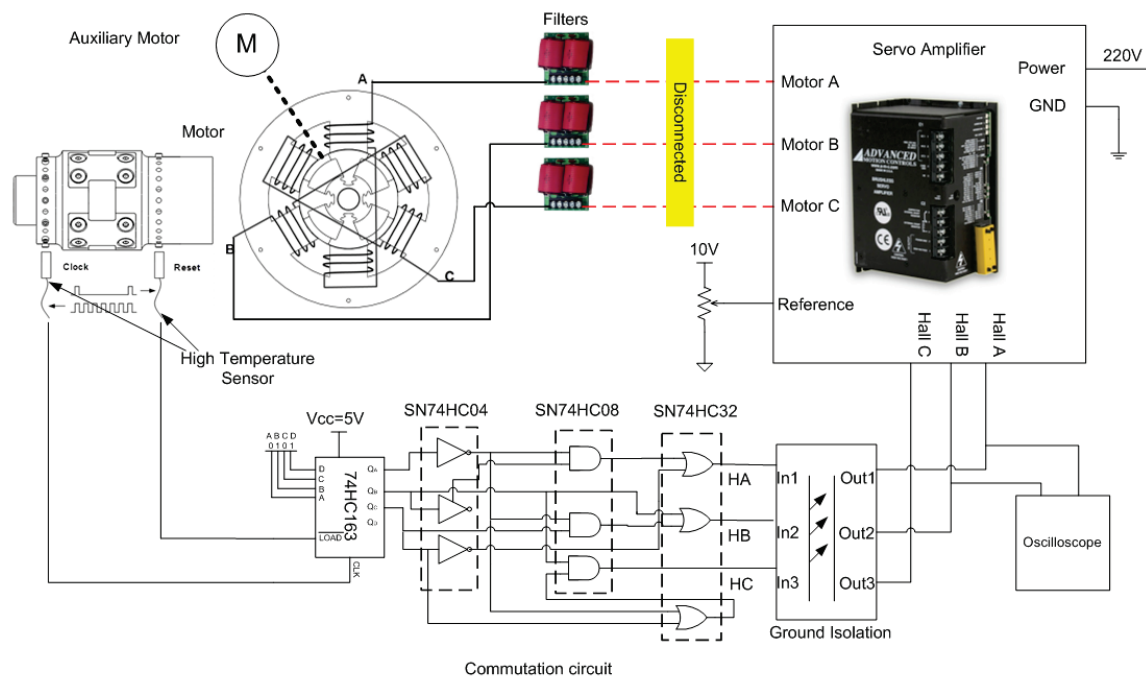

Fig. 4-15 Motor Output Disconnected and Auxiliary Motor Used

When the servo amplifier is off, the oscilloscope shows the HA and HB generated

by the digital circuit are the same as in Fig. 3-25. When the servo amplifier is activated, it does not make any difference. All of the Hall outputs stay the same with or without the servo amplifier operation. Fig. 4-16 shows two Hall outputs (HA, HB) observed at the oscilloscope. It is confirmed that the high switching frequency of PWM is NOT the source of noise that causes the problem.

Fig. 4-16 Hall Outputs Successfully Generated

The problem is caused by high temperature sensor. It is a surprise since the sensor could produce the expected Hall outputs using the auxiliary motor. But, the rotor is driven at approximately 2500 rpm and when the speed is reduced, the problem of the sensor emerges. The following figures show how the sensor problem occurs. The servo amplifier, digital circuit and auxiliary motors are stopped, leaving the high temperature sensor as the only component. By manually adjusting the position of the rotor, the high temperature sensor behavior is examined. First, when the rotor is rotated to make sensor observe at the surface of the rotor, the expected output is 6V which is the logic "high" mode(Fig.

4-17). Second, the sensor is positioned at the cap of one screw, where the output should give a logic "low" mode (Fig. 4-18). Last, as the sensor observes the edge of the screw, the output of the sensor has an abnormal behavior. The sensor does not have a constant output as expected (Fig. 4-19). This result conflicts with prior experience that normal displacement sensors, such as a Bentley Proximity Probe, will have an intermediate output between "high" and "low".


**Fig. 4-17 Sensor, Detecting the Shaft Surface**
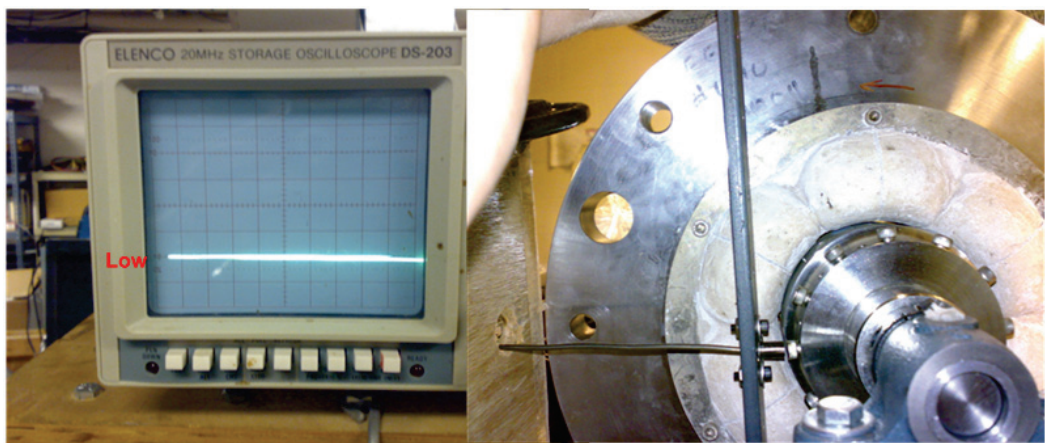
**Fig. 4-18 Sensor, Detecting the Screw Head**
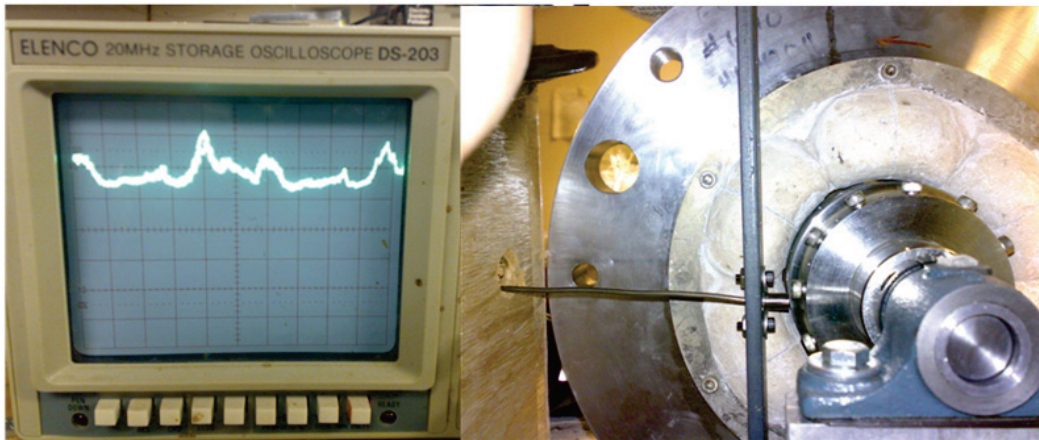
Fig. 4-19 Sensor, Detecting the Edge

This behavior leads to a serious problem. The sensor output is connected to the input of a digital circuit. There is a threshold of the input voltage above which is considered "logic high" and below which is considered "logic low". The logic circuit will change state each time the input across the threshold, so every time the edge of the screw passes the sensor, the logic state changes. One passage of the edge should have one state change only. Due to the abnormal sensor behavior, when the speed is low (ie. start up), there might be multiple passages across the threshold resulting from one passage of the edge. From the motor commutation view, the servo amplifier will consider the number of passages across the threshold the same as the number of screws passed. Hence, instead of one, multiple screws will be considered by the servo amplifier which makes the state of the motor several screws ahead from what is expected. The reason the motor motor fails to commutate correctly is mainly because of this alignment. The problem is severe at low speed since the possibility to get false counts increases. It might improve as the speed increases but it will never reach high speed operation unless it overcomes the problems at

low speed.

This high temperature probe is the only high temperature sensor available. There is nothing that may be done about this behavior except replacing the sensor. Unfortunately, these sensors are expensive.

4.4.4   Open Loop Operation

Knowing the problem is caused by the high temperature sensor in the feedback loop, a new way to make the motor work without significant change is pursued. It is confirmed that these high temperature sensors may not be used for motor commutation. An open loop approach to eliminate the use of high temperature sensors is developed.
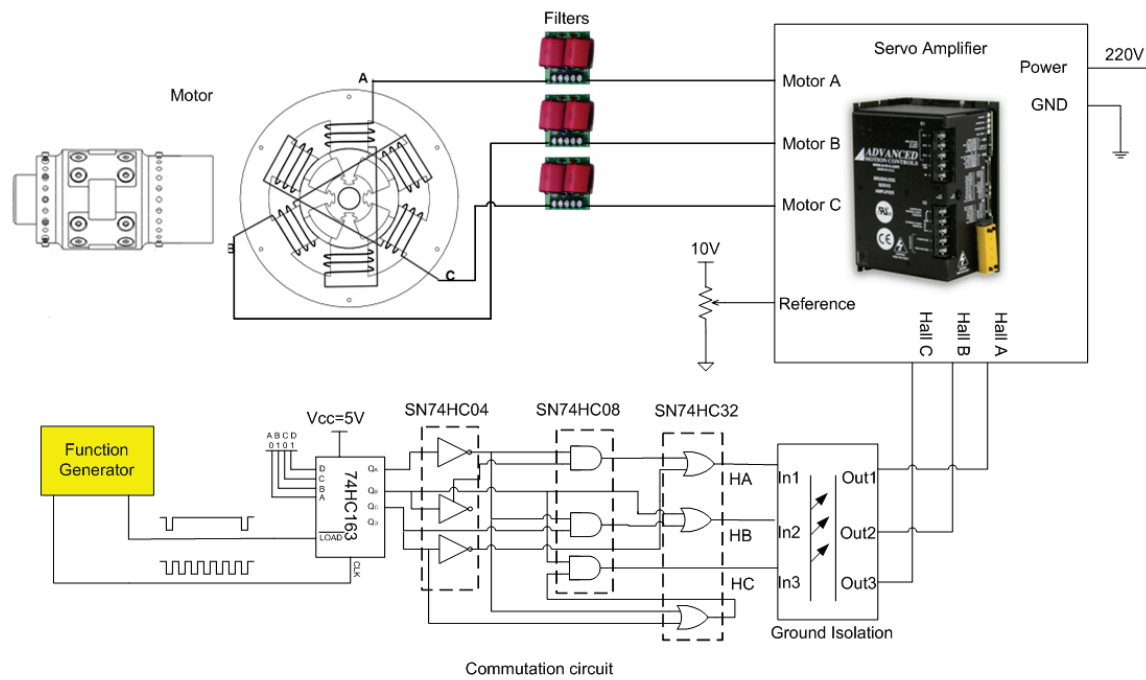

Fig. 4-20 Open Loop Motor Drive Circuit

Fig. 4-20 shows the open loop scheme. The high temperature sensors are removed and a function generator is added to generate the "Clock" and "Reset" signals. The signals are translated into three Hall outputs by the digital circuit. Then the generated HA HB and HC are inputted to the servo amplifier. Thus, instead of feedback, these three outputs become the command signals. Since there is no rotor position feedback, the servo amplifier does not measure the speed of the motor, and the servo amplifier tries to drive the motor to follow the input from the function generator.

A demonstration shows the motor can start at zero speed and be stable at low speed. With an input clock frequency of 27 Hz (135 rpm command for the motor), the motor is successfully started. The speed of the motor varies with the input frequency. The motor speed starts at approximately 135 rpm and increases to 240 rpm. There is a little slipping at the beginning, but the rotor quickly catches up and runs synchronously with the command signals.

The recorded speed and the command are shown in Fig. 4-21. It is surprising to find no steady state error. The speed of the motor tracks the command in a precise manner. A closed up plot is provided in Fig. 4-22. The highest speed tested is approximately 500 rpm. Since the rotor is unbalanced and the spin test rig is not strong enough for the higher speed test, the higher speed test may be performed once the entire assembly is finished and tested.
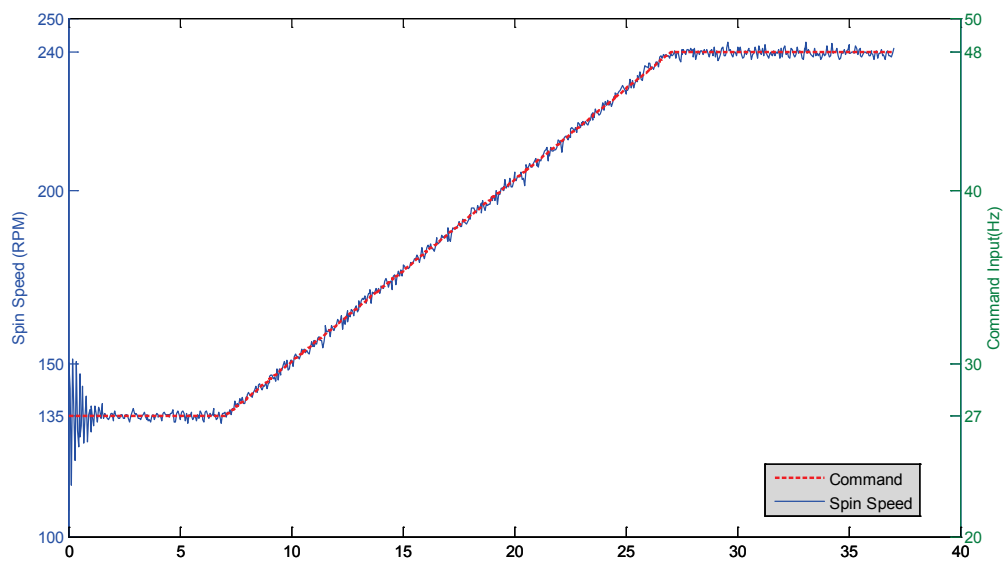
Fig. 4-21 Motor Spin Speed Response and Command
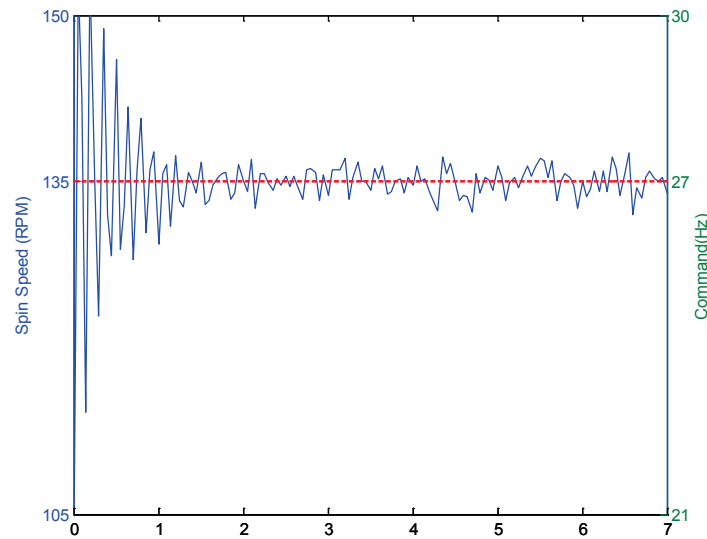
Fig. 4-22 Closed up Plot of Fig. 4-21

5.   MAGNETIC BEARING & MOTOR SYSTEM

The ultimate goal of designing this high temperature motor is to install it as a component of a high temperature magnetic bearing system. The full test rig includes two high temperature radial bearings, two radial catcher bearings, a high temperature thrust bearing and a high temperature motor (Fig. 5-1). The final assembly is in progress.

In this section, brief introduction of all the components of the system is provided. Then, the status of the full assembly and the heating system is discussed.
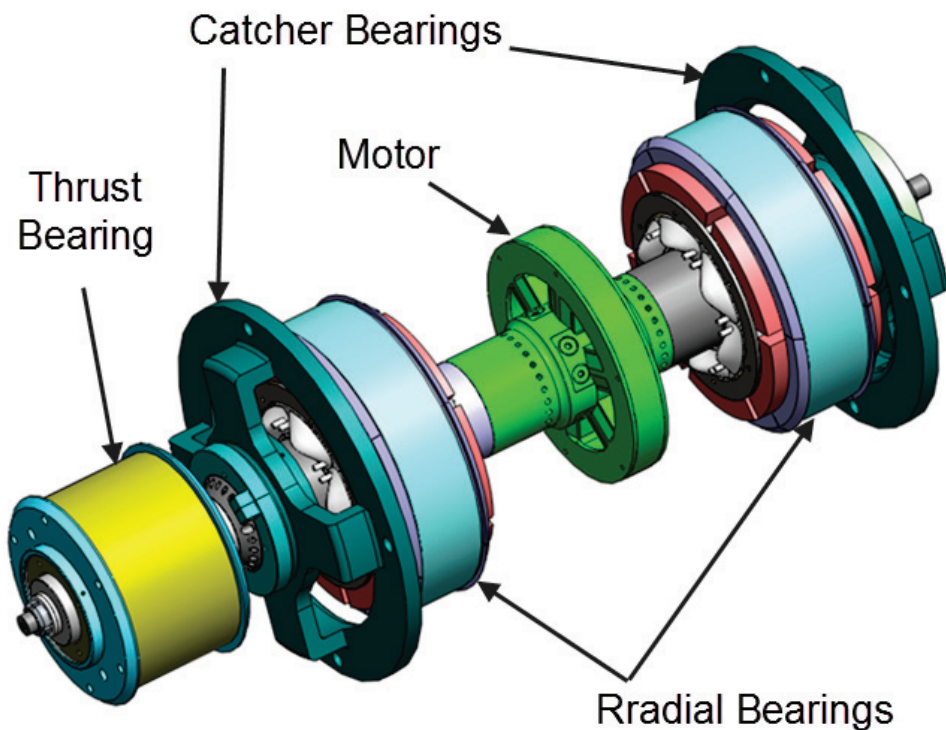

Fig. 5-1 Magnetic Bearing System

5.1 High Temperature Magnetic Bearings

There are three high temperature magnetic bearings, including two radial bearings and one thrust bearing.

5.1.1 Radial Bearings
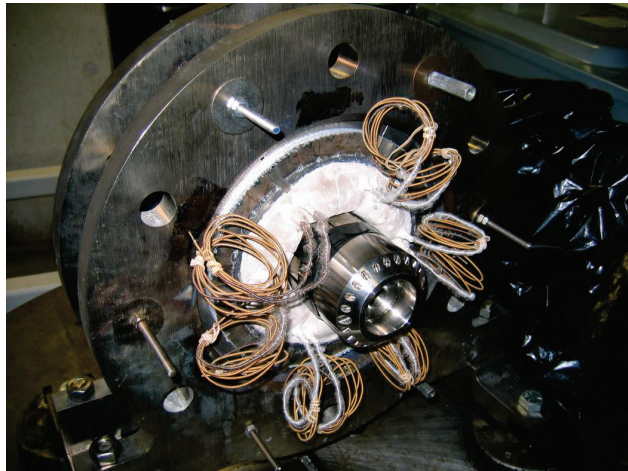
Fig. 5-2 Radial Bearing 1
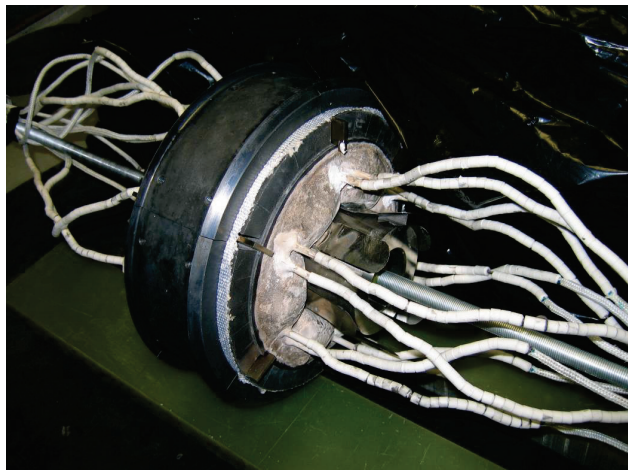
Fig. 5-3 Radial Bearing 2

Both radial bearings are fully assembled prior to the construction of the high temperature motor. These bearings are subjected to the high potential tests. Fig. 5-2 and Fig. 5-3 illustrate these two bearings. More details of the radial bearings may be found in reference [6], [7], [8],[9].and [10]

5.1.2   Thrust Bearing

A thrust bearing is designed to be positioned at the bottom of the system to levitate the entire shaft. The thrust bearing housing is treated with the same process of winding, potting (Fig. 5-4), initial curing (Fig. 5-5) and high potential test at 1000°F (Fig. 5-6).
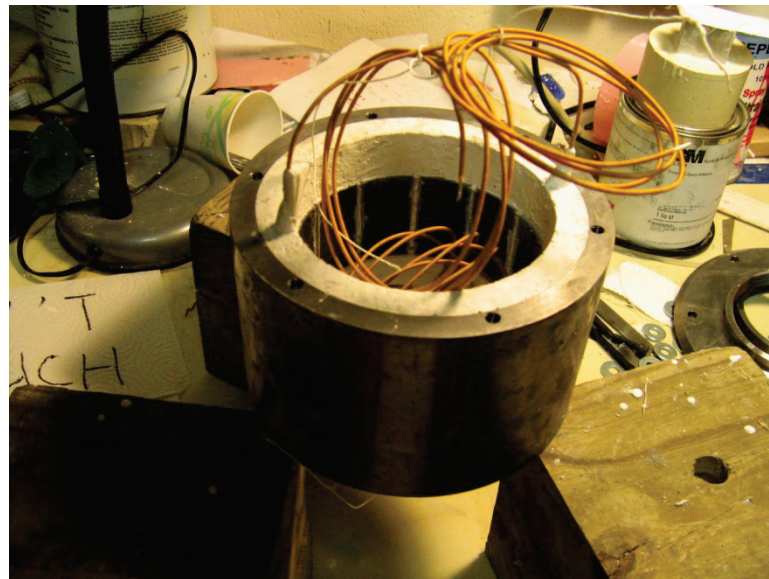
Fig. 5-4 Thrust Bearing Potting

Table 5-1 shows the high potential test results. No sign of breaking down at high

temperature implies that the coils of the thrust bearing are reliable at 1000°F.

Table 5-1 High Potential Test Results of the Thrust Bearing

Pole		High Temperature			Room Temperature		
		1000°F			74°F		
		Voltage	Current	Effective	Voltage	Current	Effective
		(V)	(µA)	Resistant(MΩ)	(V)	(µA)	Resistant(MΩ)
1	DC	500	260	1.92	500	0	inf
	AC	500	560	0.89	500	40	12.5
2	DC	500	220	2.27	500	0	inf
	AC	500	540	0.93	500	40	12.5
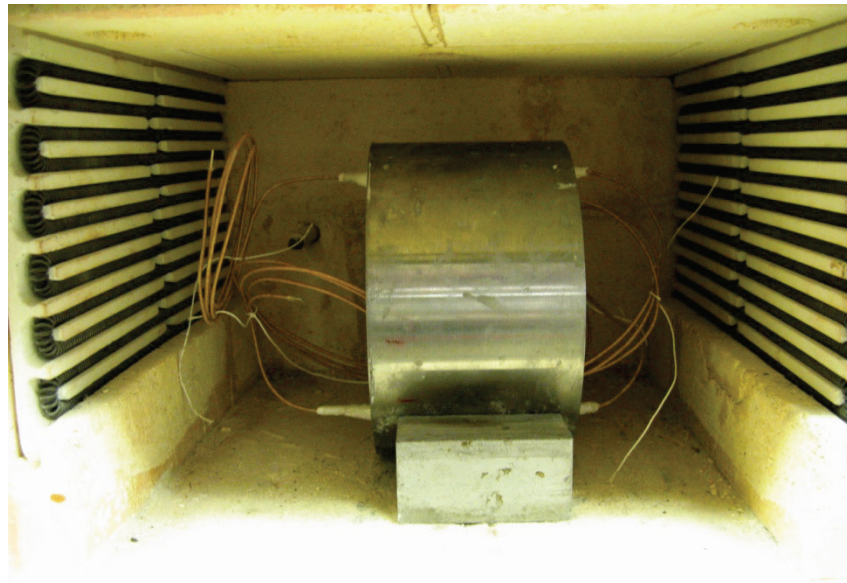
Fig. 5-5 Housing in the Oven for Initial Cure and Hipot Test
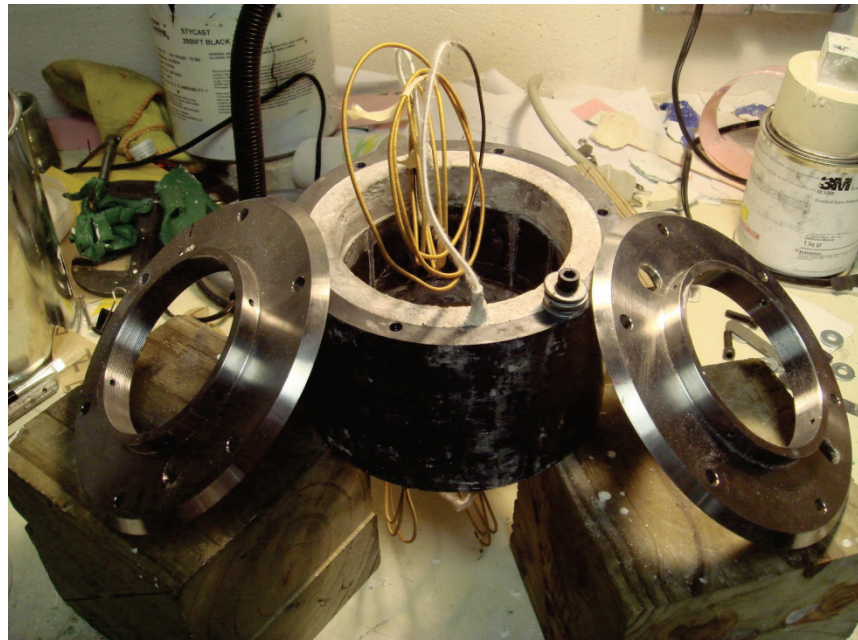
Fig. 5-6 Thrust Bearing Housing after Hipot Tests

To place the rotor in the housing, the rotor and a cover plate are fixed on a rigid structure. Six all-thread rods are used as the guide for the housing's movement. By turning the nuts, the housing is slowly moved towards the rotor (Fig. 5-7). Six nuts adjust the moving direction of the housing, which is kept parallel to the rotor axis. The six all-thread rods will be replaced with regular bolts upon the completion of the thrust bearing (Fig. 5-8).

Fig. 5-7 Rotor Inserting Procedure
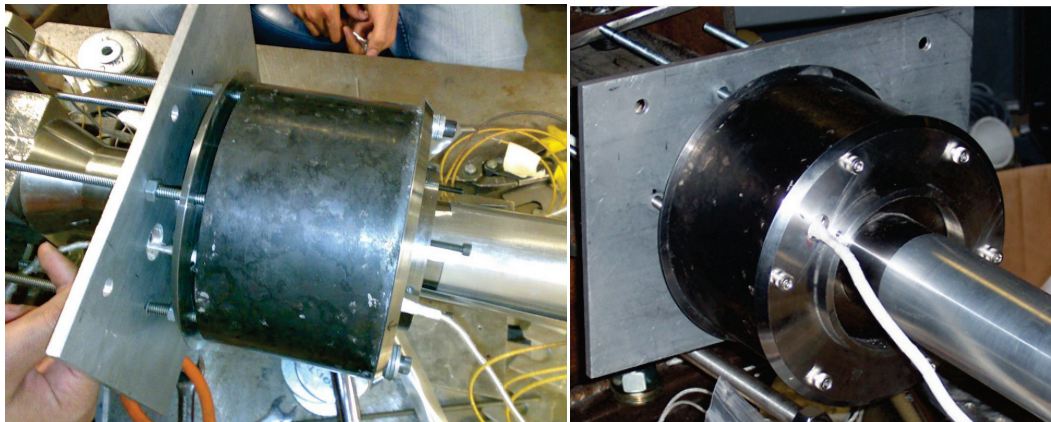
Fig. 5-8 Thrust Bearing Stator-Rotor Assembly Completed

5.1.3   Radial Catcher Bearing

Two radial catcher bearings are located next to the radial magnetic bearing. If one or more of the poles fail at the magnetic bearings, the rotor will continue running on the catcher bearing to prevent a hard landing on the poles of the magnetic bearings.

5.2   Full Assembly

The magnetic bearing will be assembled vertically in the following order from the bottom: thrust bearing, radial catcher bearing 1, radial bearing 1, high temperature motor, radian bearing 2 and radial catcher bearing 2. All of the components will be assembled in a cylinder housing and constrained by the location plates (Fig. 5-9).
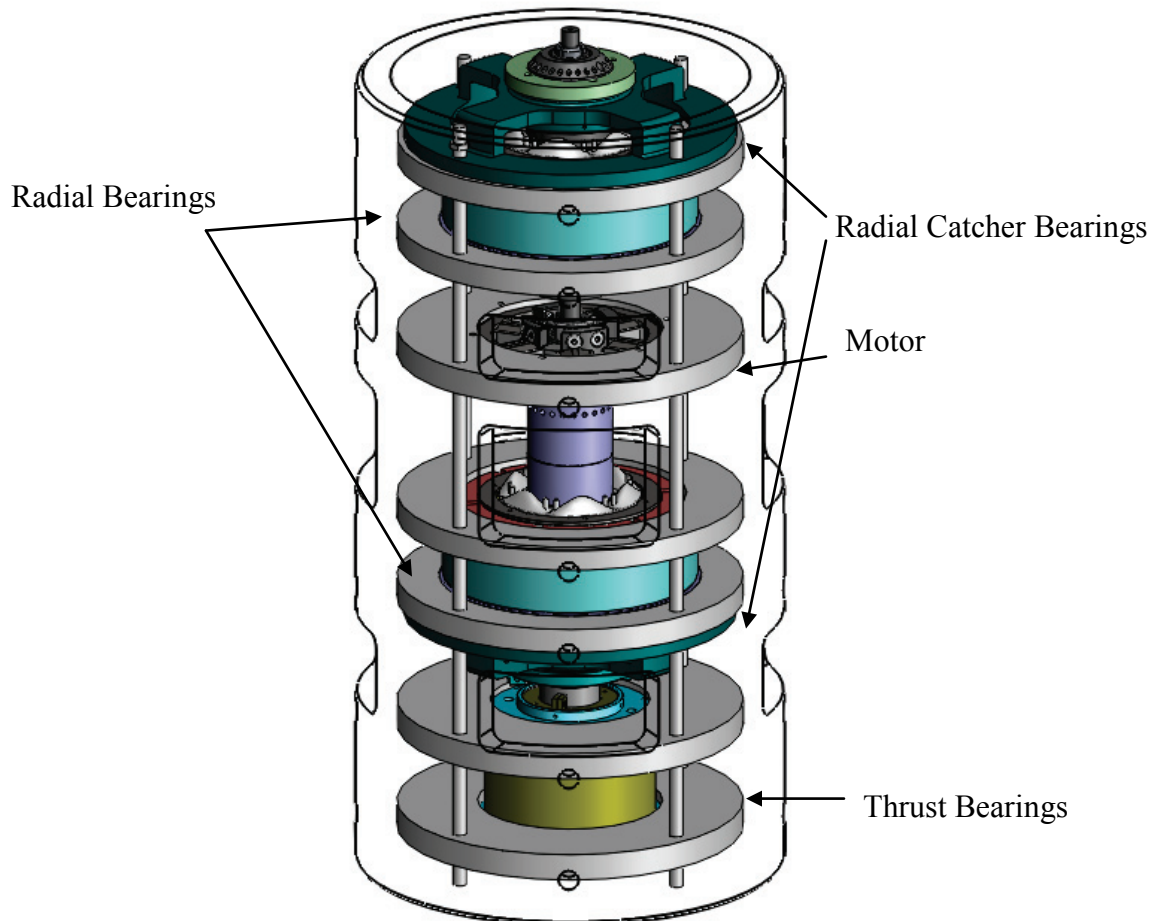
Fig. 5-9 Solidworks Model of Full Assembly

The rig will be assembled on a floor mounted stand shown in Fig. 5-10. All of the

sensors are to be mounted on the outer housing. Most of the components, including wires, thermocouples, sensors, etc, may be easily accessed through the window on the outer housing. The bearing system will operate at low temperature and low speed initially. Eventually, slow speed at moderate temperature condition tests will be conducted on the floor mounted stand. For high speed and high temperature test, the assembly will be transported to the spin pit shown in Fig. 5-11.

Fig. 5-10 Floor Mounted Stand and Housing
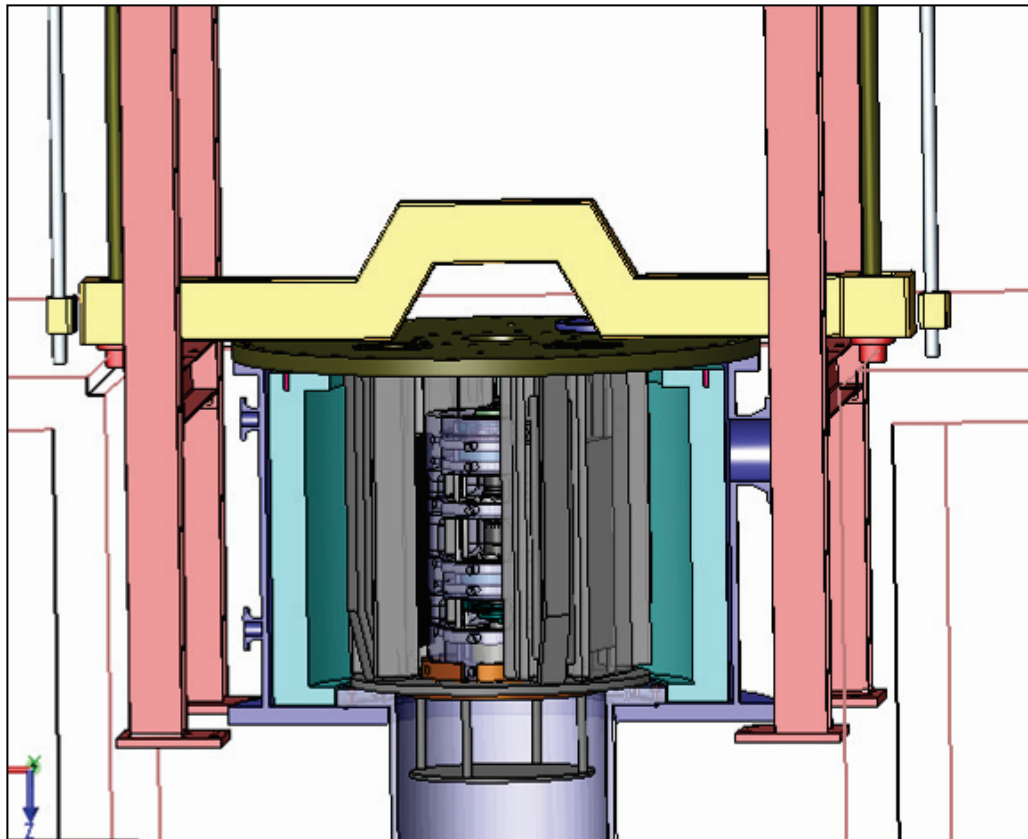
Fig. 5-11 Assembly Lowered in the Spin Pit

5.3   Heating System

For the heating system, the following components are used [11]:

- Watlow Mineral Insulated (M.I) Band Heaters (Fig. 5-12)

Quantity: 3(2 pieces split)

Power: 240V/3900W per Half

Maximum Temperatures: 1400°F

- Watlow Ceramic Fiber Radiant Heaters (Figure on p. 83)

Quantity: 4

Power: 240V / 2500W per heater

Maximum Temperature: 1800°F

- Watlow CLS216 Multi-Loop Temperature Controller(Fig. 5-13)

Fig. 5-12 Band Heaters Pair
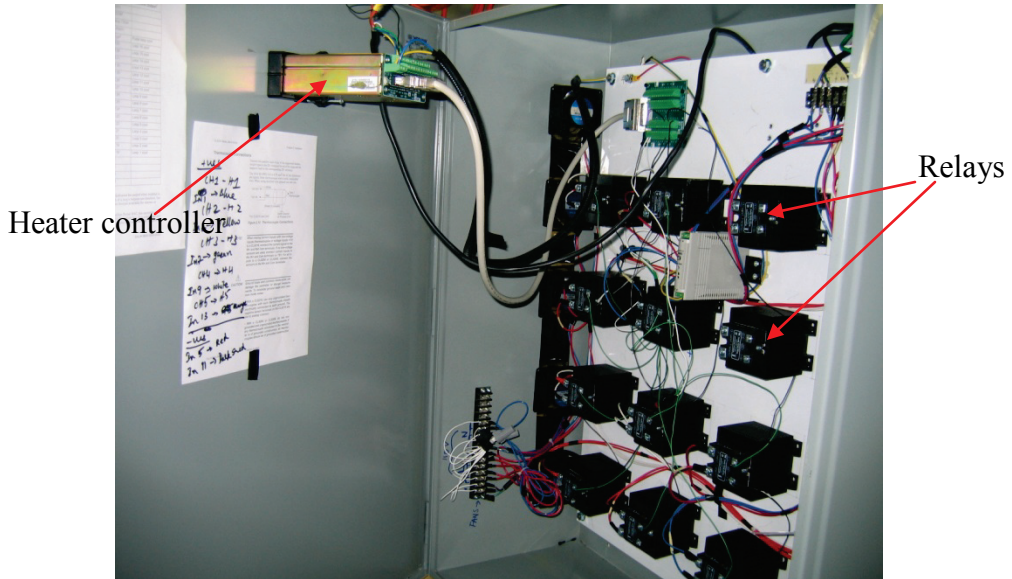
Fig. 5-13 Heater Controller and Relays

The band heaters are mounted outside of the cylinder housing at top, middle and bottom positions (Fig. 5-14).
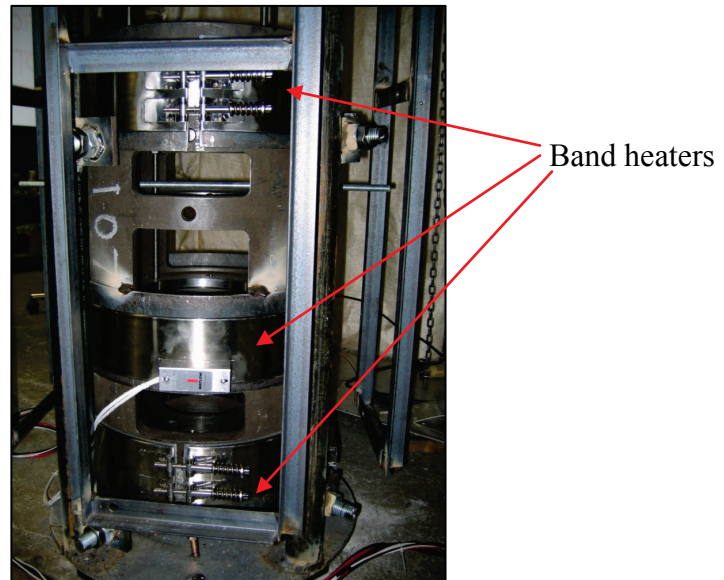
Fig. 5-14 Band Heaters Mounted on the Cylinder Housing

The designed maximum heating power is approximately 33.4 kw, which can draw about 140A current. Three pairs of band heaters are sufficient to heat the system to 1000°F. The assembly will be covered with insulation (Fig. 5-15), which is Zircar Alumina-Silica type ceramic (ECO-1200A). A heating test is performed and takes approximately 2.5 hours to heat the rig to 1000 °F only using the band heaters at 80% of the maximum heating output.
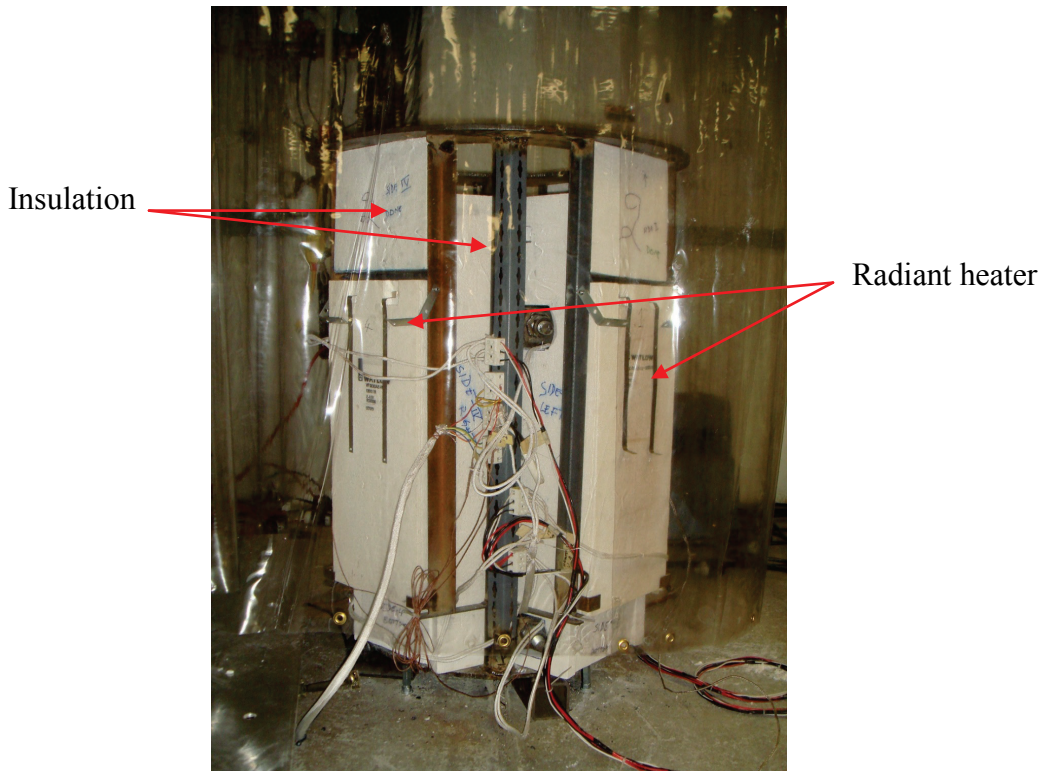
Fig. 5-15 Zircar Insulation and Radiant Heaters

6. CONCLUSION

6.1 Conclusion

A high temperature buried permanent magnet brushless DC motor, a part of the high temperature magnetic bearing system, expected to operate at 1000°F, was designed and built. High temperature permanent magnets produced by EEC were buried in the rotor. The motor stator utilized new bobbin and potting techniques developed at VCEL to survive high temperature. High potential tests were performed at both room and high temperature. Results showed no sign of deterioration.

The drive of the motor was built utilizing the AMC servo amplifier. A digital circuit was developed to provide rotor position for commutation in order to achieve closed loop motion control. Sensor problems were encountered, which caused the failure of closed loop method. After much effort to solve the sensor problems, an open loop method was found to drive the motor. The motor was demonstrated to run at low speed and room temperature with self-starting capability. The speed was also controllable using the open loop approach.

In addition, the high temperature magnetic bearing system was examined. Critical components were finished and readily for assembly. The heating system and insulation were installed. The heaters were tested to reach 1000°F within three hours.

6.2   Future Work

The future work should include the following:

- Finish assembling.

The full rig assembling is in progress.

- High temperature spin test of the motor

The motor must be tested for low speed spinning at high temperature once the rig is fully assembled. The test may be performed without magnetic bearing, with the rotor on the catcher bearings.

- Sensorless control of high temperature motor.

Sensorless control eliminates the position sensors of the motor. When temperature reaches Hall Effect sensor limitation, sensorless control is the best solution. Normally for a brushless DC motor, sensorless control obtains the rotor position by detecting the back EMF. There are several approaches such as zero crossing approach, EMF integration approach, etc that may be considered.

- Magnetic bearing controller setup.

The controllers and amplifiers for the magnetic bearing are built, but the gains of the controllers must be set.

- Full magnetic bearing system testing.

The plans for the full system test are divided into two phases. The first one will be on the floor mounted stand with a low speed (2000 rpm) at both a low temperature (room temperature) and a moderate temperature (500°F). The second one is to place the system

in the spin pit for tests of high speed (>15000 rpm) and high temperature (1000°F).

REFERENCES

[1] "High-temperature Switched-reluctance Electric Motor", Online NASA Tech Briefs, http://www.techbriefs.com/content/view/2241/32/, accessed Jun. 2009.

[2] "HoneyBee Robotics High Temperature Motor Data Sheet", http://www.honeybeerobotics.com/product-examples/components/25-hightempmotor, accessed Jun. 2009.

[3] Li ,L. Y., Kou, B. Q., Cao, J. W., 2009, "Electromagnetic Field Analysis of Axial Flux High Temperature Superconducting Synchronous Motor", *Proc. of Progress In Electromagnetics Research Symposium*, Aug. 18-21, 2009, Moscow, Russia, pp 1254~1257.

[4] Kenny A., 2007, "EEC Quarterly Report NO.6", Electron Energy Corporation Technique Report, pp 26-27.

[5] Advanced Motion Controls online analog servo amplifier B30A40AC data sheet http://www.a-m-c.com/, accessed Jan. 2009.

[6] Gandhi V. R., 2009, "High Temperature, Permanent Magnet Biased, Magnetic Bearings," M.S. thesis, Texas A&M University, Department of Mechanical Engineering, College Station.

[7] Mohiuddin, M., 2002, "Design of High Temperature High Speed Electromagnetic Axial Thrust Bearing," M.S. thesis, Texas A&M University, Department of Mechanical Engineering, College Station.

[8]   Hossain, M., 2006. "High Temperature, Permanent Magnet Biased, Homopolar Magnetic Bearing Actuator," M.S. Thesis, Texas A&M University, Department of Mechanical Engineering, College Station.

[9]   Kenny, A., Palazzolo, A., 2003, "Single Plane Radial, Magnetic Bearings Biased With Poles Containing Permanent Magnets," Transactions of the ASME, **125**, pp. 178-185.

[10]   Provenza, A., Montague, G., Jansen, M., Palazzolo, A. and Jansen, R., 2005, "High Temperature Characterization of a Radial Magnetic Nearing for Turbomachinery," Journal of Engineering for Gas Turbines and Power, **127**, pp.437-444.

[11]   "Watlow Heating Solution Manuals", http://www.watlow.com, accessed Apr. 2008.

VITA

Zhengxin Zhang was born in Chongqing, which is a beautiful city located in the southwestern of China. He was the only child in his family.

He received his Bachelor of Science degree in mechanical engineering from Shanghai Jiao Tong University, Shanghai, China in 2007. He studied at the University of Hong Kong from January 2004 to June 2004 as an exchange student. He entered the Department of Mechanical Engineering in Dwight Look College of Engineering at Texas A&M University and received his Master of Science degree in 2010. He joined the Vibration Control and Electromechanics Lab in 2008, directed by Dr. Alan Palazzolo.

Zhengxin Zhang's address is 3123 TAMU, College Station, TX, 77843. He may also be reached via email: zhangzhengxin@gmail.com.